PHOTODYNAMIC THERAPY USING CHLORIN E6 INCORPORATED MESOPOROUS SILICA NANOPARTICLES ON LUNG CANCER CELLS

by

Sena Şişman

B.S., in Biomedical Engineering, TOBB University of Econ. & Tech., 2020

Submitted to the Institute of Biomedical Engineering
in partial fulfillment of the requirements
for the degree of
Master of Science
in
Biomedical Engineering

Boğaziçi University
2024

PHOTODYNAMIC THERAPY USING CHLORIN E6 INCORPORATED MESOPOROUS SILICA NANOPARTICLES ON LUNG CANCER CELLS

APPROVED BY:

Assist. Prof. Dr. Mustafa Kemal Ruhi .....
(Thesis Advisor)

Prof. Dr. Ahmet Ademoğlu .....

Assist. Prof. Dr. Burcu Güleryüz .....

DATE OF APPROVAL: 04.09.2024

ACKNOWLEDGMENTS

I would like to extend my deepest gratitude to my thesis advisor Mustafa Kemal Ruhi for all his guidance, support, and encouragement throughout my studies. Also I am truly thankful to my dear professor Murat Gülsoy under whose leadership I began this journey.

My thanks also go out to the members of the Biophotonics Laboratory for their friendship and support with special gratitude to Ayşe ışık and Merve Yünlü for their guidance. I wish to express my gratitude to my dear friends Hazal Öztürk and Tuğçe Mutlu for their support. I also want to acknowledge with gratitude Prof. Bora Garipcan and the members of the Biomaterials Laboratory and Cell Culture Laboratory for their contributions and collaborations.

In addition, my family, the greatest presence, my dear mother Sacide, my very valuable father Turan and my precious sister Elif, I am grateful to you for adding meaning to my life and for always being my strength with your unconditional love, positivity and energy during the thesis period as well as in every other period of my life.

I am grateful to my beloved fiancé Ahmet, who has supported me in every way, motivating me with love and patience throughout this process.

This study was supported by TÜBİTAK 2210-A National MSc/MA Scholarship Program.

ACADEMIC ETHICS AND INTEGRITY STATEMENT

I, Sena Şişman, hereby certify that I am aware of the Academic Ethics and Integrity Policy issued by the Council of Higher Education (YÖK) and I fully acknowledge all the consequences due to its violation by plagiarism or any other way.

Name :

Signature:

Date:

ABSTRACT

PHOTODYNAMIC THERAPY USING CHLORIN E6 INCORPORATED MESOPOROUS SILICA NANOPARTICLES ON LUNG CANCER CELLS

Cancer threatens human health worldwide. The low selectivity and efficacy of standard therapeutic methods, including surgery, chemotherapy, and radiotherapy, may end up with recurrence and side effects. Photodynamic therapy (PDT) is minimally invasive and offers selectivity. PDT uses photochemical agents called photosensitizers (PSs) that are sensitive to light. These agents, while normally nontoxic, become activated when exposed to light and produce cytotoxic reactive oxygen species (ROS). However, these agents may have some limitations such as low water solubility, aggregation low accumulation in tumor tissue. To overcome all these problems and increase the effectiveness of PDT, drug delivery systems are researched. In this study, Mesoporous Silica Nanoparticles (MSNs) containing Chlorin e6 (Ce6) was tested by performing analyses such as dark cytotoxicity, stability, cellular uptake, photodegradation assessment under light irradiation and PDT efficacy on A-549 lung adenocarcinoma cell line. The results showed that Ce6-incorporated MSN (Ce6-MSN) has low dark toxicity, revealed significant cellular uptake and a highly effective photodynamic effect even with low energy densities. Future studies will evaluate surface modifications of Ce6-MSN to increase cellular uptake, and create a more stable structure. Another future obejective would be to focus on loading different PSs to increase PDT effect and see the effectiveness of the treatment in in vivo studies.

Keywords: Photodynamic Therapy, Cancer, Mesoporous Silica Nanoparticles, Chlorin e6

ÖZET

AKCİĞER KANSERİNİN FOTODİNAMİK TERAPİSİ İÇİN KLORİN E6 YÜKLÜ MEZOGÖZENEKLİ SİLİKA NANOPARTİKÜLLER

Kanser dünya çapında insan sağlığını tehdit eden bir hastalıktır. Cerrahi, kemoterapi ve radyoterapi gibi standart tedavi yöntemlerinin düşük seçiciliği ve etkinliği, tekrarlama ve yan etki riskini artırır. Fotodinamik terapi (PDT) çevredeki sağlıklı dokulara en az zararı vererek seçicilik sağlayan minimal invaziv bir tedavi yöntemidir. PDT, fotosensitizan denen ışığa karşı duyarlı fotokimyasal ajanlar kullanır. Bu ajanlar normalde toksik değilken ışığa maruz kaldığında aktifleşir ve hücre ölümünü tetikleyen reaktif oksijen türleri (ROS) üretebilir. Ancak, fotosensitizanların düşük suda çözünürlük, agregasyon ve tümör dokusunda toplanamama gibi bazı sınırlandırmaları olabilir. Bütün bu sorunların önüne geçmek ve PDT'nin etkinliğini artırmak için nanoparçacık tabanlı ilaç taşınım sistemleri kullanılabilir. Bu çalışmada, Klorin e6 (Ce6) içeren Mezogözenekli silika nanopartiküller (MSN'ler) A-549 akciğer adenokarsinomu hücre hattında karanlık sitotoksisite, stabilite, hücresel alım, ışık altında fotodegradasyon değerlendirmesi ve PDT etkinliği gibi analizler yapılarak test edildi. Sonuçlar, Ce6 içeren MSN'nin (Ce6-MSN) düşük karanlık toksisitesini, önemli hücresel alımını ve düşük enerji yoğunluklarında bile oldukça etkili bir fotodinamik etki gösterdiğini ortaya çıkarmıştır. Sonraki çalışmalar, hücresel alımı artırmak, daha kararlı bir yapı oluşturmak için Ce6-MSN'nin yüzey modifikasyonlarını değerlendirecektir. Gelecekteki bir diğer hedef ise, PDT etkisini artırabilmek için Ce6 ile birlikte farklı fotosensitizanlar yüklenmesine odaklanmak ve tedavinin etkinliğini in vivo çalışmalarda görmek olacaktır.

Anahtar Kelimeler: Fotodinamik Terapi, Kanser, , Mezogözenekli silika nanopartiküller, Klorin e6

TABLE OF CONTENTS

ACKNOWLEDGMENTS iii
ACADEMIC ETHICS AND INTEGRITY STATEMENT iv
ABSTRACT v
ÖZET vi
LIST OF FIGURES ix
LIST OF SYMBOLS xi
LIST OF ABBREVIATIONS xii
1. INTRODUCTION 1
1.1 Motivation and Objectives 2
2. BACKGROUND 3
2.1 Lung Cancer 3
2.2 Photodynamic Therapy 3
2.3 Photosensitizer 5
2.4 Chlorin e6 6
2.5 Nanoparticles in Photodynamic Therapy 7
2.6 Mesoporous Silica Nanoparticles 8
3. MATERIALS AND METHODS 10
3.1 MSN Synthesis 10
3.2 APTES-mediated amino-functionalization of mesoporous silica nanoparticles 11
3.3 Loading Ce6 into the MSNs 12
3.4 Characterization of Nanoparticles 12
3.5 Cell Culturing 12
3.6 Dark Toxicity Measurement 14
3.7 Comparison of the Dark Toxicities 15
3.8 PDT Experiments 15
3.9 Comparison of PDT Efficacy of free Ce6 and Ce6-MSN 18
3.10 Cellular Uptake Experiment 18
3.11 Evaluating The Contribution of Singlet Oxygen in Cellular Toxicity . . 21

3.12 Photodegradation Assessment under Light Irradiation 22
3.13 Photodynamic Stability Experiment 22
3.14 Statistical Analysis 23
4. RESULTS 24
4.1 Characterization of Nanoparticles 24
4.2 Dark Toxicity Result 26
4.3 Determination of loaded amount of Ce6 into the Ce6-MSN 27
4.4 PDT Experiment Result 29
4.5 Comparison of PDT Efficacy of Free Ce6 and Ce6-MSN 30
4.6 Cellular Uptake 31
4.7 Primary Singlet Oxygen Mechanism 32
4.8 Photodegradation Assessment Under Light Irradiation 35
4.9 Comparison of the photostability of free Ce6 and Ce6-MSN 36
5. DISCUSSION 37
6. CONCLUSION 39
REFERENCES 40

LIST OF FIGURES

Figure 2.1	The mechanism of PDT.	4
Figure 2.2	Diagram illustrating the PDT's photochemical process.	4
Figure 3.1	(a) MSN (b) APTES-mediated amino-functionalization of MSN (c) Ce6-MSN.	10
Figure 3.2	(a) Synthesis process of MSN (b) After the washing steps of MSN.	11
Figure 3.3	The A-549 lung cancer cells with 10x magnification. Scale bar: 200 μm.	13
Figure 3.4	Illustration of dark toxicity experiments.	14
Figure 3.5	96 well plate for PDT experiment.	16
Figure 3.6	PDT Experimental Setup, with 660 nm LED light source	17
Figure 3.7	Representation of a 96 well plate seeding plan for an experiment on comparison of PDT efficacy.	18
Figure 3.8	Representation of a six-well plate seeding plan for an experiment on cellular uptake.	19
Figure 3.9	Falcon tubes both before (left) and after (right) the extraction of accumulated Ce6.	20
Figure 3.10	Representation of a six-well plate seeding plan for an experiment on singlet oxygen experiment.	21
Figure 4.1	Size Distribution result of MSN.	24
Figure 4.2	MSNs SEM images demonstrates the physical characterization.	25
Figure 4.3	Results of MTT assay for A549 cells incubated with varying concentrations of Ce6-MSN. Every group's data was normalized with respect the corresponding no treatment value. Significant difference marked by (**) ($p < 0.01$). Significant difference marked by (***) ($p < 0.001$).	26
Figure 4.4	The standard curve of Ce6.	27
Figure 4.5	Absorbance spectrum of Ce6.	28

Figure 4.6 Dark toxicity results for A549 cells treated with Ce6 (10.8 μg/mL) and Ce6-MSN (50 μg/mL). Every group's data was normalized with respect to the corresponding no treatment value (ns:no significant difference). 29

Figure 4.7 MTT assay results for A549 cells incubated with Ce6-MSN and light, only light and only Ce6-MSN. Light irradiation was performed with 100 mW/cm^2 and at 660 nm. Data for each group were normalized to the corresponding no treatment. Significant difference marked by (**) ($p < 0.01$). Significant difference marked by (***) ($p < 0.001$). 30

Figure 4.8 MTT assay results after the incubation of A549 cells with Ce6 and Ce6-MSN and light irradiation performed with 100 mW/cm^2 and at 660 nm. Each group was exposed to light for 1 minute. Significant difference marked by (**) ($p < 0.01$). 31

Figure 4.9 Cellular uptake results of Ce6 and Ce6-MSN.Significant difference marked by (***) ($p = 0.0007$). 32

Figure 4.10 MTT assay results of 50 mM Sodium Azide in A-549 cells in dark condition. Data for the group were normalized to no treatment. 33

Figure 4.11 MTT assay results of A-549 cells after incubation with and without sodium azide, light irradiation performed with 100 mW/cm^2 and at 660 nm for 5 minutes. Data for each group were normalized to the corresponding untreated controls.Significant difference marked by (**) ($p < 0.01$). 34

Figure 4.12 Absorbance change of Ce6 and Ce6-MSN under 660 nm with time. 35

Figure 4.13 Photostability of Ce6 and Ce6-MSN during 14 days, absorbance at 660 nm. 36

LIST OF SYMBOLS

$^1O_2$	Singlet oxygen
mW/cm^2	Milliwatts per Square Centimeter
μg/mL	Microgram per Mililiter
O_2	Oxygen
mM	Millimolar
mL	Milliliter
nm	Nanometer
μL	Microliter

LIST OF ABBREVIATIONS

ANOVA	Analysis of Variance
APTES	(3-Aminopropyl)triethoxysilane
Ce6	Chlorin e6
Ce6-MSN	Chlorin e6 incorporated Mesoporous Silica Nanoparticles
CM	Cell Membrane
CTAB	Cetyltrimethyl Ammonium Bromide
DI water	Deionized Water
DLS	Dynamic Light Scattering
DMEM	Dulbecco's Modified Eagle Medium
DMSO	Dimethyl Sulfoxide
DNA	Deoxyribonucleic Acid
EPR	Enhanced Permeability and Retention
FA	Folic Acid
FBS	Fetal Bovine Serum
FDA	US Food and Drug Administration
HA	Hyaluronic acid
LED	Light Emitting Diode
MPR	Microplate Reader
MSN	Mesoporous Silica Nanoparticles
MTT	3-[4,5-dimethylthiazol-2-yl]-2,5 diphenyl tetrazolium bromide)
NIR	Near Infrared Radiation
NSCLC	Non-Small Cell Lung Cancer
PBS	Phosphate Buffered Saline
PDT	Photodynamic Therapy
PEG	Polyethylene glycol
PS	Photosensitizer
ROS	Reactive Oxygen Species
SCLC	Small Cell Lung Cancer

SEM	Scanning Electron Microscope
SLN	Silica Nanoparticles
TEOS	Tetraethyl Orthosilicate
UV-Vis	UV-Visible Spectroscopy
WHO	World Health Organization

1. INTRODUCTION

An article by the World Health Organization (WHO) stated that by 2025, there will be 35 million new cancer cases, up from 20 million in 2022. This growth is largely attributed to economic development, population growth, and aging. Additionally, the cancer rates are strongly influenced by lifestyle factors such as alcohol and tobacco use, and obesity. Among environmental risk factors, air pollution has also emerged as a significant contributor [1].

Lung cancer is considered a commonly diagnosed and aggressive type of cancer [2]. The output of the study conducted by the International Agency for Research on Cancer GLOBOCAN focusing on cancer incidence and mortality which underlines that 1.8 million deaths in 2020 recorded regarding to lung cancer [3]. Current cancer treatment methods are surgery, chemotherapy, radiation, immunotherapy, hormone therapy, and more [4].

Being among the mentioned treatment options, PDT is a minimally invasive treatment method for cancer and some non-cancerous disorders, which uses light, endogenous molecular oxygen, and a photosensitizer (PS) [5]. Each component is harmless on its own, but when PS is exposed to light, photochemical reactions create reactive oxygen species (ROS), which cause cytotoxicity [6]. ROS cause tumor cells to die by necrotic, autophagic, or apoptotic processes [7]. One critical point here is that the PS should be activated by light with wavelength that PS has high absorption. Typically PSs that have absorption in the red or NIR are preferred since they can penetrate relatively deeper into tissue [5].

PDT is primarily effective for tumors in surface due to light's restricted ability to penetrate deeper tissues. Adequate tissue oxygenation is also necessary for optimal production of ROS, which can be difficult in the hypoxic environments commonly found in certain tumors. Accurate timing and power density of light are essential for treatment

effectiveness with potential limitations due to inflammation and photosensitivity in the treated area [8]-[10]. The above features presents the potential of PDT while also emphasizing its specific constraints in clinical settings.

1.1 Motivation and Objectives

Compared to conventional therapies like surgery or radiation, PDT offers minimal invasiveness, and selectivity [11]. Additionally, PDT can be repeated without accumulating toxicity, which makes it appropriate for recurring tumors or chronic conditions [12].

To enhance treatment outcomes, PDT can be used either alone or in conjunction with other therapies including topical treatments or systemic drugs [13]. Because of these qualities, PDT is a potentially useful method, especially for conditions such as superficial cancers, precancerous lesions, and some non-malignant conditions.

This study aims to assess PDT on A549 cell line using Ce6 incorporated mesoporous silica nanoparticles (MSN).

2. BACKGROUND

2.1 Lung Cancer

Lung cancer is a common and aggressive disease which is one of the greatest cause of death worldwide. Although smoking is the primary risk factor, environmental exposures (such as air pollution, arsenic, radon, biomass fuels, and industrial carcinogens) lead to lung cancer related mortality [14].

There are two common types of lung cancer; non-small cell lung carcinoma (NSCLC) and small-cell lung carcinoma (SCLC) [15]. Although SCLC is less common, it is known as a more aggressive type of lung cancer. Treatment methods and approaches vary depending on the degree of the cancer. For instance, surgery is typically performed to remove the tumor along with some of the healthy tissue that surrounds it in the early stages of NSCLC. In case surgery is not applicable, chemotherapy and radiotherapy can be applied. However, these treatment methods are not always effective and cause side effects [16].

Considering the limitations of the treatment options and, possible side effects, research into new treatment methods has increased rapidly. PDT, being a solid example of methods among those use nonionizing radiation and can provide selective therapy, thus it has aroused great interest in cancer treatment.

2.2 Photodynamic Therapy

PDT, a light-mediated technique, employs photosensitizers (PS) exposed to a suitable light wavelength. In addition to treating cancer, it is frequently utilized in the medicine to find alternative solutions to ocular or dermatological conditions [17].

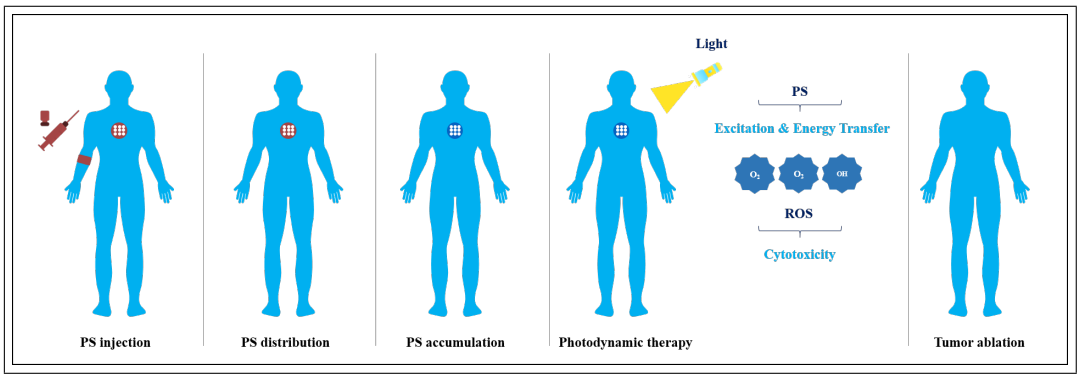

Figure 2.1 The mechanism of PDT.

The components of PDT (PS, light, and oxygen) are not toxic on their own, but the irradiation of PSs with light leads to a photochemical reaction that results in the formation of ROS, mainly singlet oxygen, which causes cell death through apoptosis or necrosis [18].

Minimally invasiveness, distinct mechanism of action, and low side effects made PDT a popular cancer treatment method [19]. PDT is a therapy method that can be used repeatedly and in combination with other therapies [20].

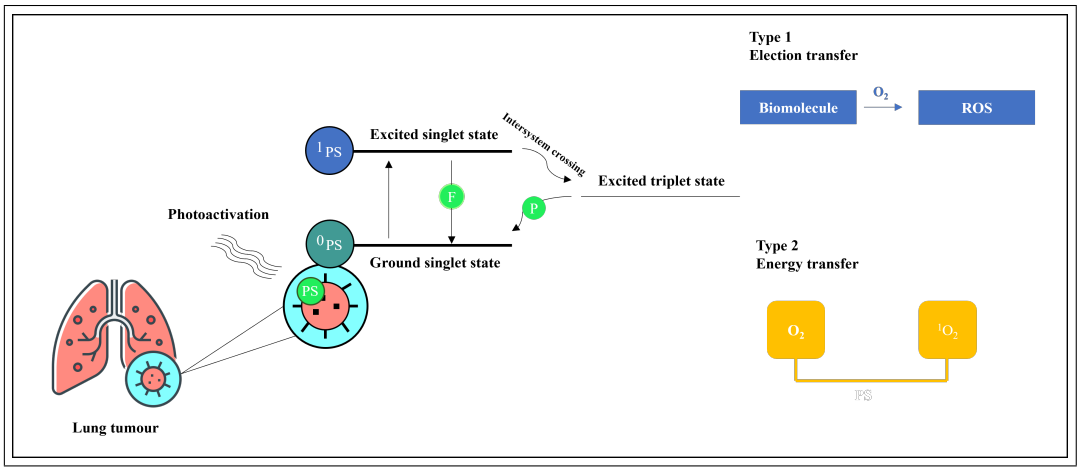

Figure 2.2 Diagram illustrating the PDT's photochemical process.

There are two types of photochemical reaction occurred. Free radicals are generated during Type I reactions when PS gives or receives electrons from the biomolecules. These reactions result in the production of ROS subsequently in the chemical process. Through a triplet-state energy transfer mechanism, singlet oxygen ($^1O_2$) is produced in a Type-2 reaction. Following light absorption, the photosensitizer transfers energy to molecular oxygen. This excitation causes the production of reactive singlet oxygen which initiate oxidative harm and cell damage. This reaction may result in selective elimination of cancer cells or pathogens [21].

2.3 Photosensitizer

Photosensitizers play a vital role in PDT by absorbing light and producing ROS that eliminate cancer cells. The selection of photosensitizer has significance in the success of therapy. An ideal photosensitizer should have high absorbance in the therapeutic window, which is defined as being between 600 and 850 nm due to deeper penetration [19].

An important requirement for photosensitizers is to accumulate selectively in tumor tissue to minimize damage to surrounding tissue. Therefore, PSs are frequently used with delivery systems to increase their accumulation into tumors [22]. Also, PS should be biocompatible, and be able to rapidly clear from healthy tissue. Another favorable feature of PSs is that they should produce ROS effectively and have a high quantum yield. In the absence of light, it should have minor intrinsic PS toxicity and modest dark toxicity [23].

The porphyrin-based first generation photosensitizers had low selectivity to malignant tissue and they had absorption around 600 nm light, which has limited penetration in tissues. For these reasons, second generation photosensitizers have emerged [24].

2.4 Chlorin e6

A chlorophyll derivative second generation PS, Chlorin e6 (Ce6) is well-known for its capacity to generate ROS in response to light exposure, which has potential in PDT applications. Ce6 has ability to absorb light near-infrared (NIR) region between 660-690 nm particularly. Comparing this absorption range to photosensitizers that absorb in the visible spectrum, it enables deeper tissue penetration [25].

Ce6 causes significant damage to cellular components and the destruction of targeted cells. By focusing on particular cells or tissues, Ce6 can improve selectivity of PDT and reduce harm to healthy tissues. Furthermore, Ce6 often has minimal systemic toxicity, enhancing patient safety and minimizing adverse effects [26].

Ce6 was used by Sheleg et al. to conduct a clinical evaluation of PDT for pigmented melanoma skin metastases. The authors draw the conclusion that PDT with Ce6 is efficient and well tolerated for treating cutaneous metastases from melanoma [26].

Yuhua Li et al. carried a study using Ce6 to evaluate the anticancer efficacy of PDT on SW480 cells. The authors showed that Ce6-PDT administration could limit cell proliferation, lower the capacity of SW480 cells to migrate and form colonies, and dose-dependently increase ROS generation and apoptosis. These results could serve as experimental support to the clinical application of Ce6-PDT for treating colorectal cancer [27].

Additionally, Jiaxing Yang et al. synthesized a carrier that was able to preferentially target the homogeneous human gastric cancer cells by coating silica nanoparticles (SLN) with cell membrane (CM) made from human gastric cancer cell line which is called SGC7901. The authors showed that CM/SLN/Ce6 can serve as a potential vehicle for efficient tumor-targeted PDT of gastric cancer because of its modification, which allows it to kill SGC7901 cells in vitro and in vivo [28].

Subramaniyan et al. produced Ce6 photosensitizer conjugated silica NPs with folic acid (FA) linkage for PDT treatment to breast cancer cells. MDA-MB-231 cells exhibited high uptake of the biocompatible silica-Ce6-FA that had been synthesized. Under laser irradiation, the silica-Ce6 connection was robust and produced ROS. The created nanoparticles were successfully taken by cancer cells. The results of the cytotoxicity test showed that, when laser therapy was used, silica-Ce7-FA killed MDA-MB-231 cells more effectively than free Ce6. As a result, targeted PDT could be implemented with these designed particles [29].

Ce6 has benefits over other agents and is well known as a PDT agent that is frequently used in both experimental and clinical applications. However, research on this PS is ongoing to overcome drawbacks, including irreversible degradation, poor solubility in aqueous solutions, and quick light bleaching [28].

2.5 Nanoparticles in Photodynamic Therapy

Nanoparticles have unmatched aspects and various advantages those distinguished it for improving PDT. For example, nanoparticles can provide encapsulation in photosensitizing agents and enhance their delivery to targeted areas. Systemic exposure and adverse effects can be reduced by using targeted delivery whereas concentration of photosensitizer at the tumor area is increased [30].

Nanoparticles can preserve photosensitizers from degradation before reaching the target area. The photosensitizers' continued activity and efficacy throughout the PDT procedure is guaranteed by this protection. It is possible to reengineer nanoparticles, thereby they release photosensitizers under controlled conditions in response to external stimuli like light or pH shifts. By using a controlled release, the medicinal substances are only released when necessary [31].

Nanoparticles usually benefit from the improved permeability and retention (EPR) effect, a situation causing molecules to accumulate in tumor tissue and fa-

cilitates PS carriers' entry and retention in tumor tissue. The localization to the target area is significant in both PDT and other cancer treatments [31].

In a study, the authors performed on glioblastoma U87 cells to evaluate the photodynamic efficiency of nanoparticles formed with silica and titanium. In contrast to PEGylated nanoparticles, APTES modification made the nanosystems more efficient for PDT. The study showed that regardless of the type of nanoparticles with silica and titanium, Ce6 seemed to be localized inside the vesicles. ROS production was quite high for both. Efficient uptake of nanoparticles by U87 cells and high ROS production indicated that silica nanoparticles-APTES-Ce6 could be considered as potential nanoparticles for PDT [32].

2.6 Mesoporous Silica Nanoparticles

Mesoporous silica nanoparticles (MSNs) have advantageous structural characteristics, which include high surface area, stability, adjustable pore size, and easy functionalization of the particle surface [33].

Because of their huge surface area and clearly defined porous structure, MSNs enable a significant loading of photosensitizers onto or within the nanoparticles. This indicates that the photosensitizer can reach the target place at a higher concentration. The photosensitizers can be released gradually and under control thanks to porous structure of MSN. This may contribute to the drug's long-term maintenance of therapeutic levels in the desired location [34].

Targeting ligands or antibodies that link exclusively to cancer cells can be added to MSNs to improve PDT treatment specificity and lessen harm to nearby healthy tissues. Additionally, the mesoporous structure can shield photosensitizers from photobleaching or premature degradation, increasing PDT's effectiveness overall [34].

In a study, the influence of combining PS and MSN on PDT was analyzed,

and the benefits of this combination were highlighted. To summarize the key findings, PS-MSN hybrid nanosystems demonstrated the following capabilities: reduction or elimination of cytotoxicity under dark conditions, improved solubility and stability in physiological media, enhanced selectivity and internalization in cancer cells, which promotes antitumor PDT activitiy with lower amounts of PS and ensures safe clinical use concerning PS in solution [35].

Due to the side effects and high recurrence rates of chemotherapy, Sanghyo and his colleagues applied chemotherapy and PDT together by creating nanoparticles that target cancer cells. For this purpose, the authors conjugated hyaluronic acid (HA) to MSNs to specifically target cancer cells to enhance the efficacy of chemotherapy and PDT, they loaded HA-MSNs with doxorubicin and Ce6. The authors showed in the study that the drugs added to MSNs were more effective than the drugs used alone [36].

In another study, a MSN-based nanocarrier was synthesized to deliver both Ce6 and doxorubicin for a combination cancer therapy. When formed in this manner, A549 was effective against cancer cells nanoparticles that entered somehow increased the cellular reactive oxygen species level in cells by 17-fold. However, it has been shown how important MSNs are for effective anticancer therapy when combined with photosensitizers [37].

This study was conducted to investigate the efficacy of Ce6-incorporated MSNs on A-549 cells in terms of PDT efficacy, stability and cellular uptake.

3. MATERIALS AND METHODS

3.1 MSN Synthesis

MSNs were synthesized as described previously in the literature [38]. In short, 7.5 mL of deionized water was mixed with 1.057 mL of NH_4OH on a magnetic stirrer. To get the mixture to 30 mL, 21.44 mL of deionized water was put in while magnetic stirring was done at 500 rpm and 40°C. The mixture was then given 0.058 g of cetyltrimethylammonium bromide (CTAB) and allowed to dissolve. After adding 482 μL of ethanol and 118 μL of TEOS to the mixture progressively, the temperature was increased to 60 °C. After two hours of vigorous stirring, the nanoparticles precipitated from the mixture. The solution containing the nanoparticles was then subjected to three ethanol washes using a centrifuge and a sonicator. The formed nanoparticles were dissolved in 20 mL of ethanol, followed by the addition of 20 μL of hydrochloric acid (HCl). The mixture was then stirred at 500 rpm and 60°for 3 hours. Finally, the MSNs were centrifuged, sonicated, and washed three times with ethanol.

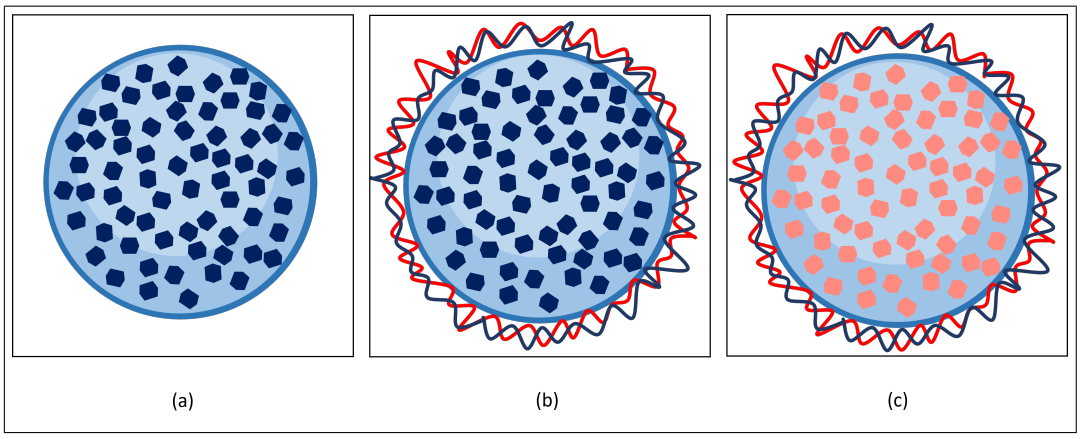

Figure 3.1 (a) MSN (b) APTES-mediated amino-functionalization of MSN (c) Ce6-MSN.

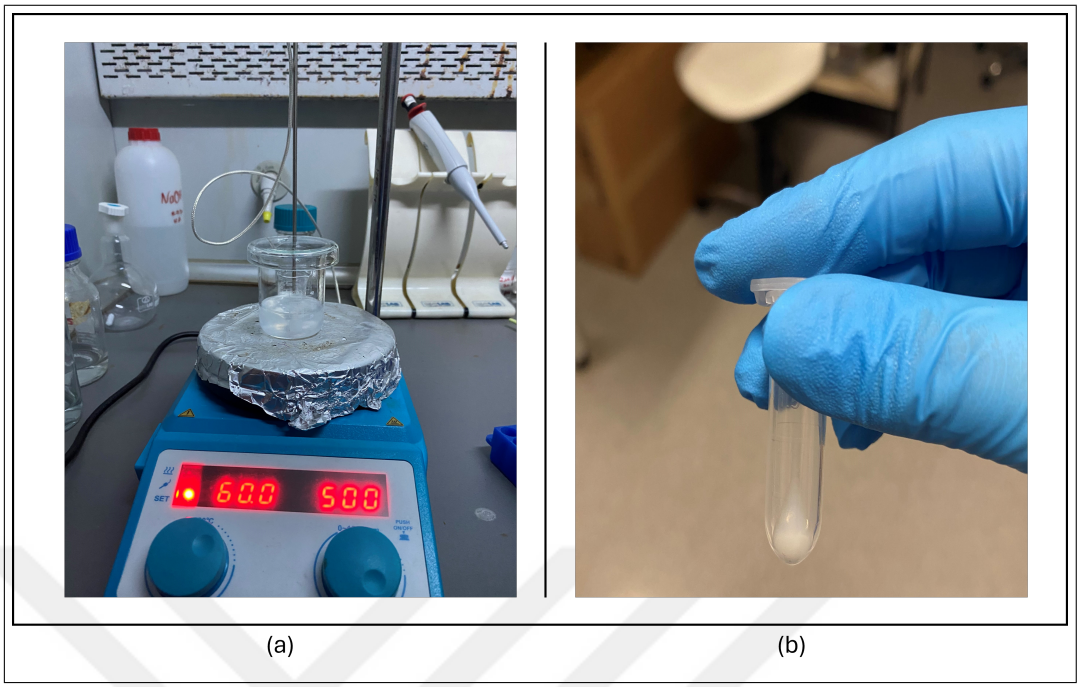

Figure 3.2 (a) Synthesis process of MSN (b) After the washing steps of MSN.

3.2 APTES-mediated amino-functionalization of mesoporous silica nanoparticles

3-Aminopropyltriethoxysilane (APTES) is mainly employed for functionalizing MSNs across various applications. The addition of APTES to an MSN solution causes the silanol groups (-Si-OH) on the silica surface to establish covalent connections with it, covering the MSN surface with amino groups. These amino groups facilitate covalent bonding or electrostatic interactions with photosensitizers, thereby enhancing the loading capacity of these therapeutic agents within the mesopores. This surface modification technique not only boosts the stability of the nanoparticles but also prevents incorporated molecules from aggregating within MSN pores, guaranteeing a homogeneous distribution [39]. MSNs were dissolved in 15 mL of ethanol for this study, and 20 μL of APTES was thereafter added to the MSNs gradually. The mixture was stirred using a magnetic stirrer at 500 rpm while maintaining a temperature of room temperature for a duration of 24 hours. After that, ethanol was used to wash the mixture three times.

3.3 Loading Ce6 into the MSNs

2 mg/ mL Ce6 was dissolved entirely in 20 mL DMSO and ethanol mixture by vortexing and magnetic stirring. Then the MSN that was synthesized was added. For 24 hours, the mixture was stirred at 500 rpm while it was at room temperature. The synthesized nanoparticles were then washed three times with deionized water, and kept in the freezer for use in future experiments.

3.4 Characterization of Nanoparticles

The synthesized MSNs were kept in a incubator in 60 °C for 24 hours and the density of formed MSNs was measured with a sensitive weighing device. After dissolving about 15 mg of synthesized MSN in 1.5 mL of ethanol, the mixture was homogenized by sonicating it. Scanning Electron Microscopy (SEM) was used to determine the shapes and morphology of the synthesized nanoparticles. The size distribution was identified through the application of the dynamic light scattering (DLS) technique, which examines light intensities produced by the Brownian motion -the movement and collision of molecules - . DLS generates a size distribution profile by examining the diffusion coefficients of several sample particles; this profile usually displays the mean size and size variability [40]. A standard curve was generated using the absorbance values ranging from 5 - 500 μg/mL Ce6 at 655 nm using a microplate reader (MPR) (BIO-RAD / iMark) to calculate the Ce6 concentration in synthesized Ce6-MSNs.

3.5 Cell Culturing

For this study, the A-549 human lung adenocarcinoma cells were cultured. First, the cells were thawed in a 37 °C water bath. To provide complete medium, 10% fetal bovine serum (FBS) and 1% Penicillin-Streptomycin were added to Dulbecco's Modified Eagle Medium (DMEM). After being transferred to T-25 flasks, the flasks

were incubated at 37 °C with 5% CO_2. The medium was regularly discarded and new medium was added. After the cells reached between 80% and 90% confluence, the old medium was aspirated, sterile PBS washed, and trypsin-EDTA solution was added for cell detachment.

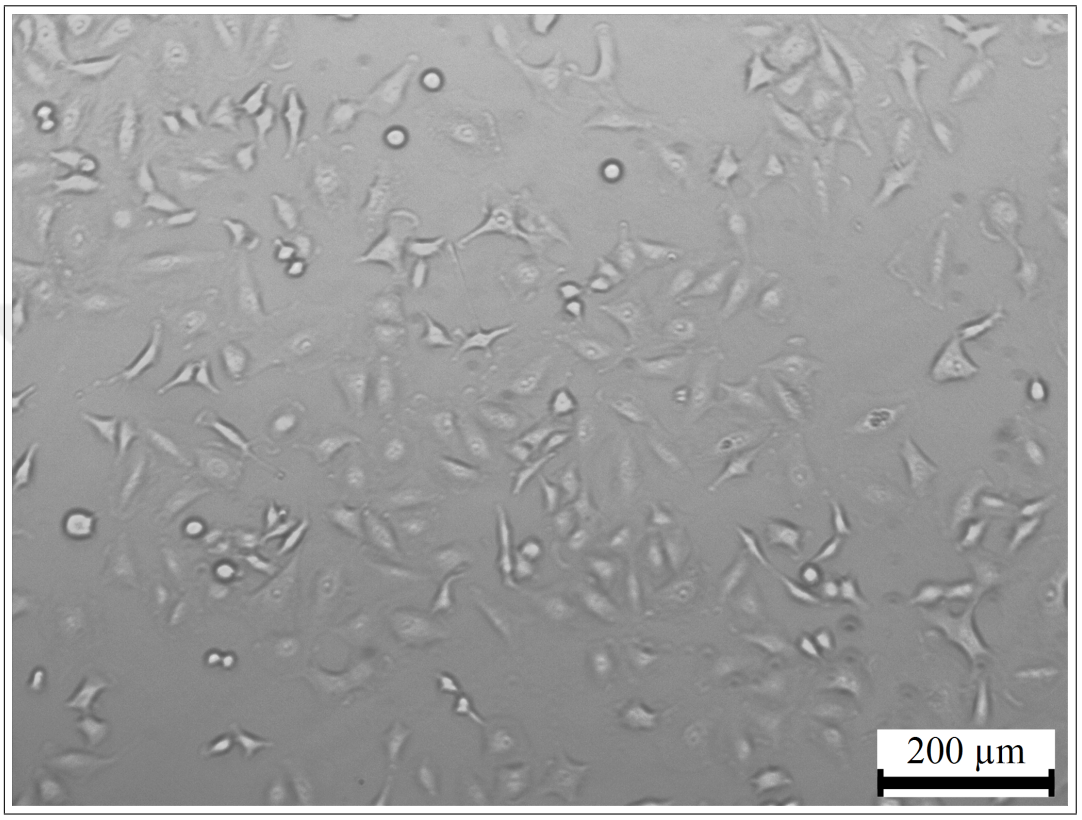

Figure 3.3 The A-549 lung cancer cells with 10x magnification. Scale bar: 200 μm.

3.6 Dark Toxicity Measurement

In dark toxicity experiments, 1x10^4 cells were seeded into the wells of a 96-well plate. Seven groups were used to represent varying concentrations of Ce6-MSN, and a no treatment group was also included. The cells were incubated for 24 hours before being treated for 2 hours with 5, 10, 25, 50, 100, 250, and 500 μg/mL of Ce6-MSN.

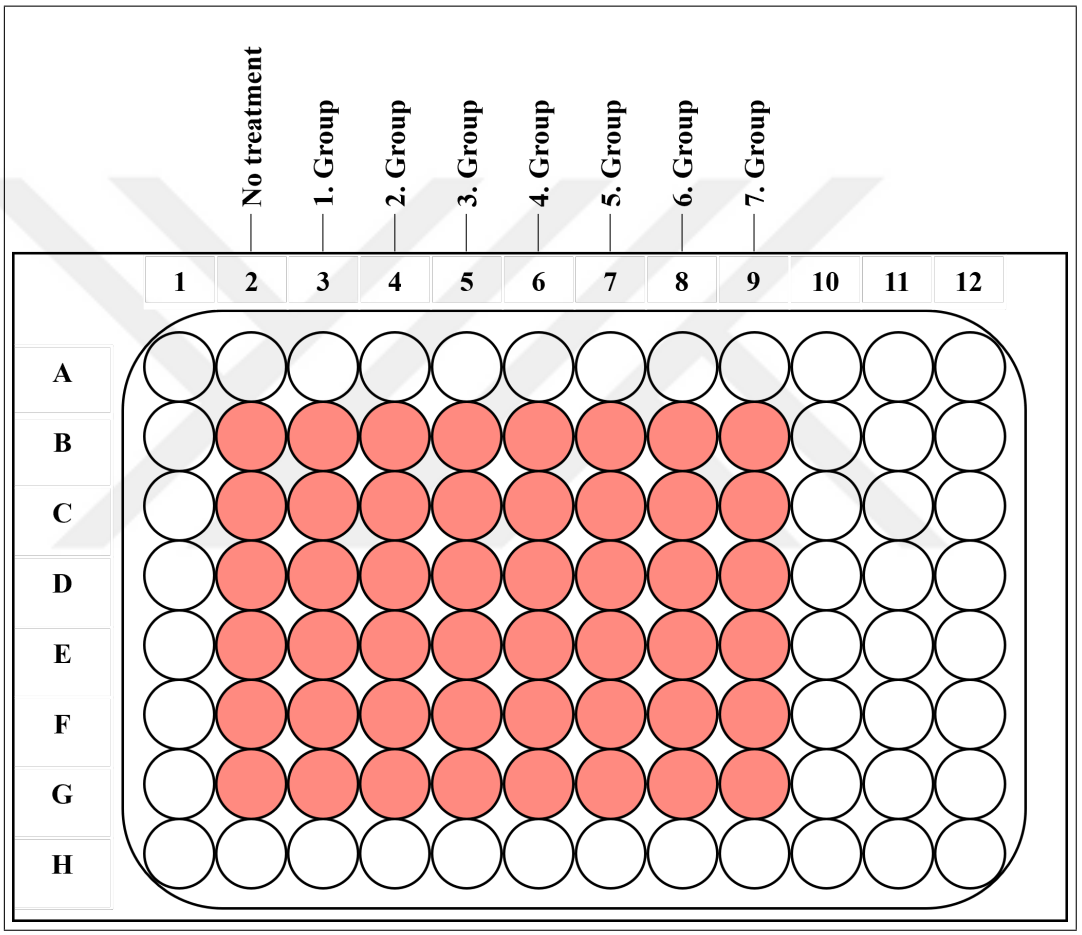

Figure 3.4 Illustration of dark toxicity experiments.

After 2 hours of incubation, PBS was used three times to wash each well. New medium was added to wells and incubated again for 24 hours. Then, MTT (3-(4.5-dimethylthiazol-2-yl)-2.5-diphenyltetrazolium bromide) was applied to each well to evaluate the cytotoxicity of drug-loaded mesoporous silica nanoparticles. After approximately 3 hours, MTT was removed and 100 μl of DMSO was added to each well. Results were obtained using MPR. Three independent repeats were performed.

3.7 Comparison of the Dark Toxicities

In this experiment, the dark toxicities of Ce6 and Ce6-MSN at the same concentrations were compared. The Ce6 concentration to be used alone was calculated by the absorbance value from the standard curve graph. DMSO was used as solvent. After 24 hours of incubation of the seeded cells, 50 μg/mL Ce6-MSN and 10.8 μg/mL Ce6 was added to the cells. The cells were incubated for two hours, and then they were three times washed with PBS. And the medium was added to the wells. Following a 24-hour incubation period, MTT was applied as mentioned before. Two independent repeats were performed.

3.8 PDT Experiments

Cells were seeded into 96-well plates and divided into ten groups: no treatment, light only without Ce6-MSN, dark with Ce6-MSN, 15 seconds, 30 seconds, 1 minute, 2.5 minutes, 5 minutes, 10 minutes and 20 minutes of light exposure. The light and dark groups were then supplemented with 50 μg/mL of Ce6-MSN following a 24-hour incubation period. After incubating for two hours, the wells were washed three times using PBS before being incubated with fresh medium. With the exception of the dark group and no treatment, the cells were exposed to a continuous wave (CW) 660 nm LED light source (ThorLabs M660L4) at a power density of 100 mW/cm^2. The MTT assay was performed a day later. Three independent repeats were performed.

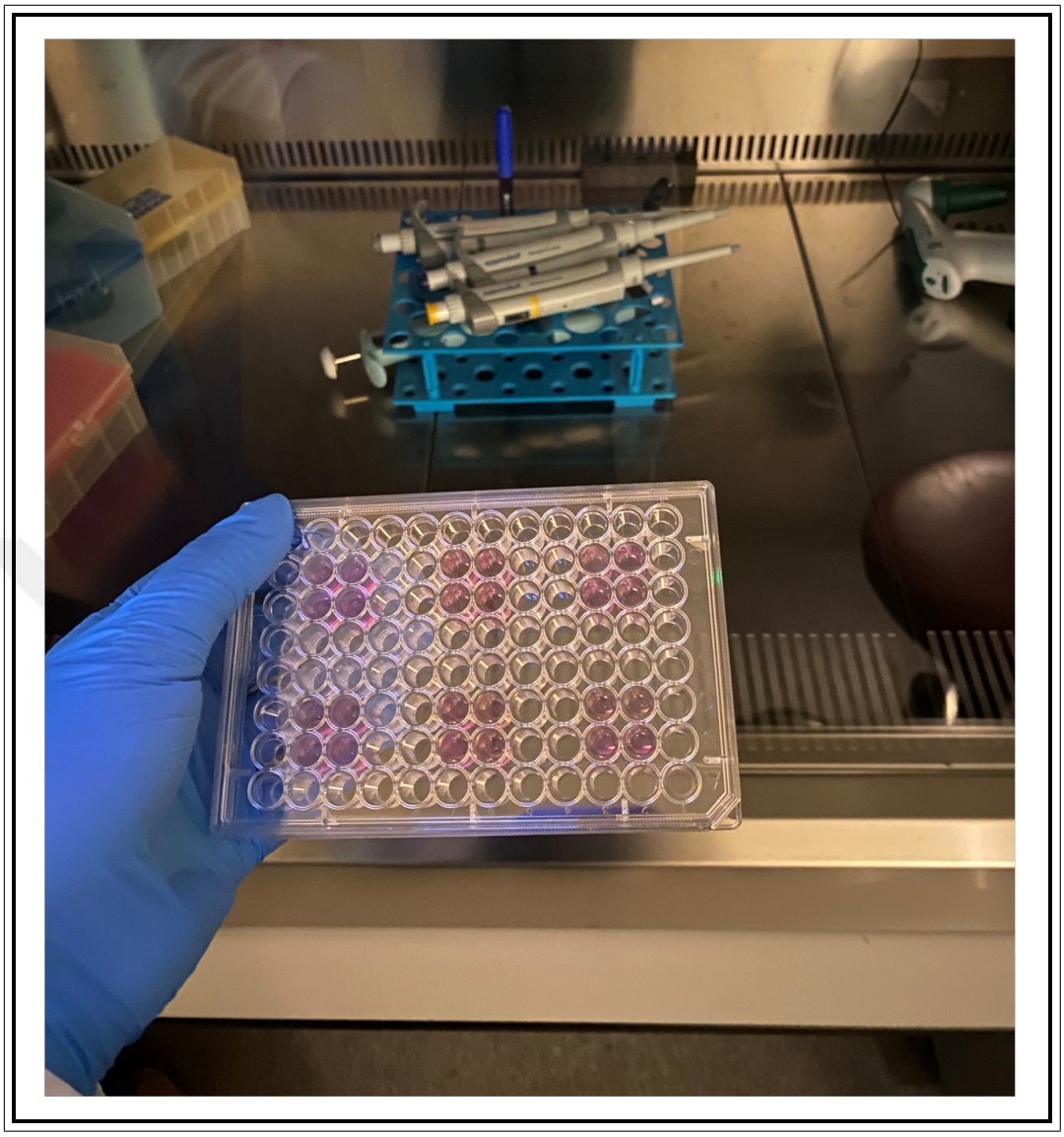

Figure 3.5 96 well plate for PDT experiment.

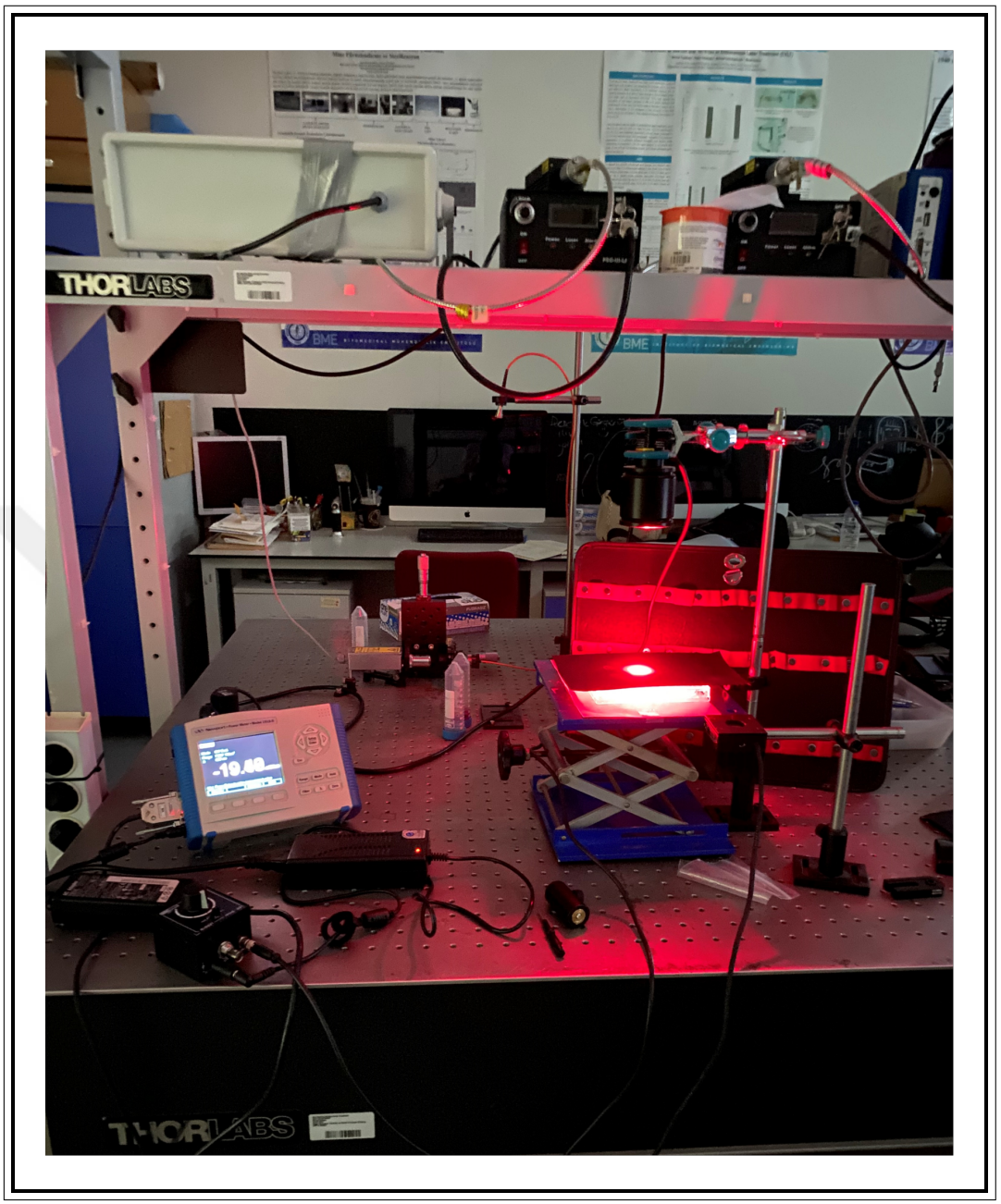

Figure 3.6 PDT Experimental Setup, with 660 nm LED light source

3.9 Comparison of PDT Efficacy of free Ce6 and Ce6-MSN

This experiment was conducted to compare the efficacy of Ce6 alone and Ce6 with MSN under light. After 24 hours of incubation, 10.8 μg/mL Ce6 and 50 μg/mL Ce6-MSN were added to the seeded cells. After waiting in the incubator for 2 hours, 100 mw/cm^2 was applied under a continuous wavelength 660 nm LED light source. For this experiment, the cells were kept under light for 1 minute. Then, they were kept in the incubator for another 24 hours. MTT was performed and the results were obtained.

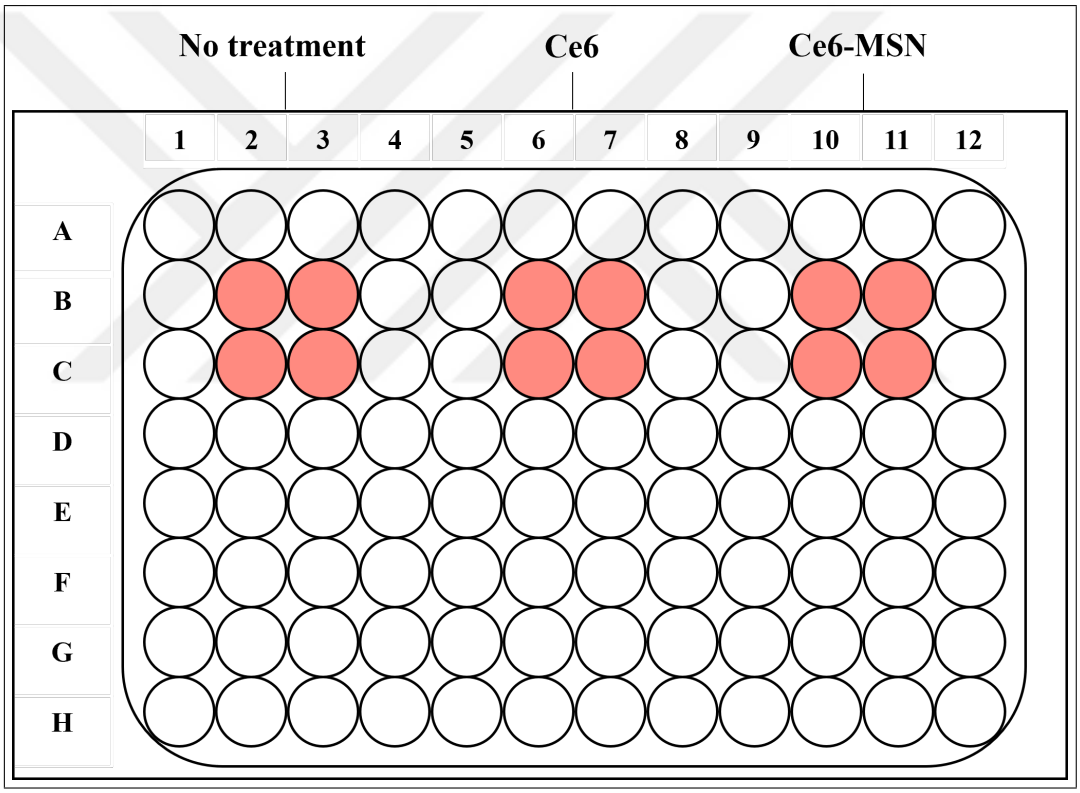

Figure 3.7 Representation of a 96 well plate seeding plan for an experiment on comparison of PDT efficacy.

3.10 Cellular Uptake Experiment

The cellular uptake of Ce6 and Ce6-loaded mesoporous silica nanoparticles (Ce6-MSN) was assessed in accordance with methodologies established in prior research [41].

In short, 2 x 10^5 cells were seeded into each well of a 6-well plate and incubated for 24 hours.

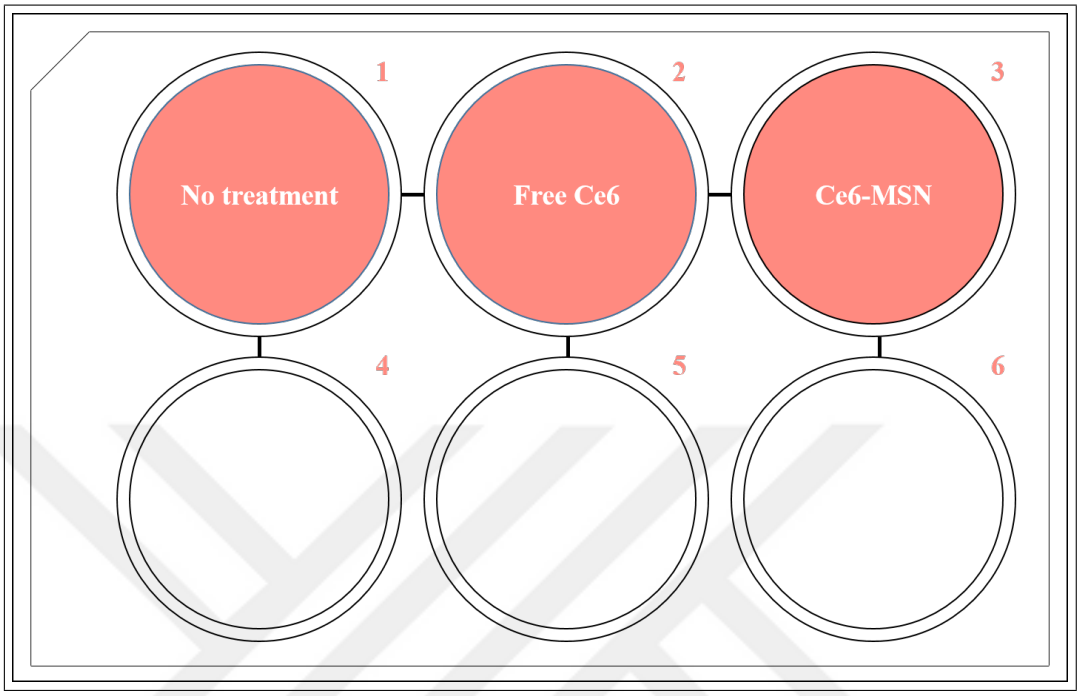

Figure 3.8 Representation of a six-well plate seeding plan for an experiment on cellular uptake.

After that, the wells were filled with predetermined amounts of free Ce6 and Ce6-MSNs, and incubated for two hours. Following incubation, cells were detached from the surface utilizing Trypsin-EDTA, collected in falcon tubes, and centrifuged for five minutes at 1000 rpm. Then, the cells were washed with PBS. To extract Ce6 from the cells, a 90% acetone solution containing 500 μL was added to each falcon tube and deionized water mixture. The supernatants were transferred to a 96-well plate, and absorbance was measured at 655 nm using microplate reader. The absorbance values were used to quantify Ce6 based on the standard curve equation, referenced as Eq. 3.1.

$$y = 0.0037x + 0.422 \qquad R^2 = 0.9544 \tag{3.1}$$

where y = *absorbance of supernatants and* x = *concentration of Ce6*

To determine the amount of Ce6 in 1 μL of the supernatants, the equation will

be referenced as Eq. 3.2.

$$q = x.\frac{M_{Ce_6}}{10^6} \tag{3.2}$$

where q = Ce6 amount in 1 μl of supernatants M_{Ce6} = molecular weight of Ce6.

To adjust for the 500 μL solution volume, the absorbance values were multiplied by 500, assuming this factor remained uniform across all tubes. This adjustment standardizes the absorbance values to a consistent volume. The Ce6 uptake per cell was then calculated by dividing the adjusted absorbance values by the number of cells in each well. This approach quantitatively assesses the uptake of free Ce6 and Ce6-MSNs by the cells under the experimental conditions.

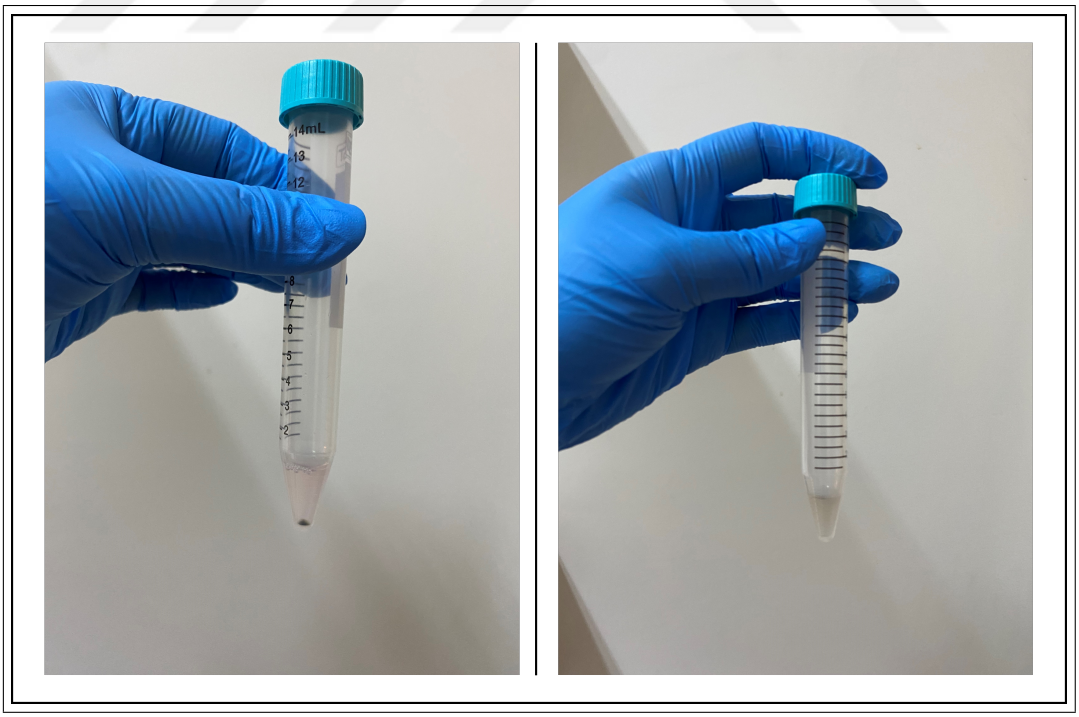

Figure 3.9 Falcon tubes both before (left) and after (right) the extraction of accumulated Ce6.

3.11 Evaluating The Contribution of Singlet Oxygen in Cellular Toxicity

In experimental conditions, an oxygen-depleted atmosphere is created using sodium azide. The effects of PDT under hypoxic conditions (low oxygen levels) and how oxygen availability affects the effectiveness of the treatment by reducing or scavenging the amount of oxygen are evaluated. Thus, if singlet oxygen is the method by which PDT kills cells, then incorporating sodium azide into the medium during PDT stops cell death [42].

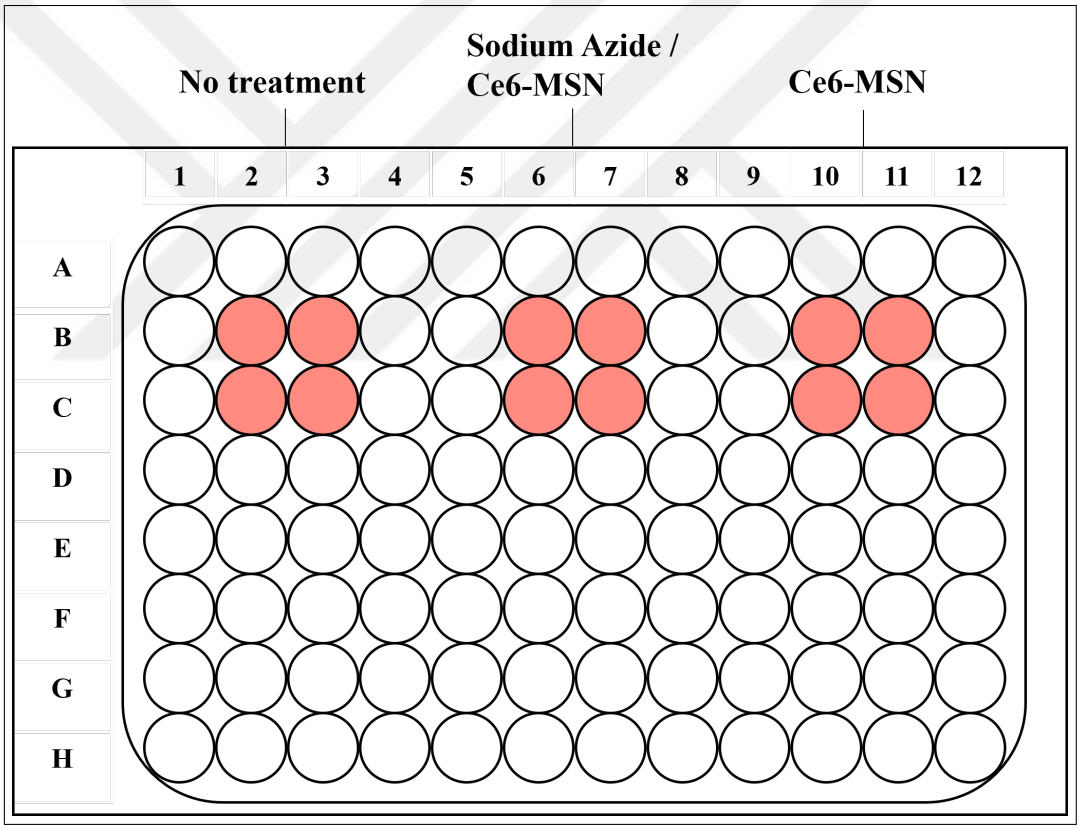

Figure 3.10 Representation of a six-well plate seeding plan for an experiment on singlet oxygen experiment.

Firstly, it was established what sodium azide's harmless concentration was in A-549 cells.

The experimental groups as follows:

- No treatment

- Ce6-MSN + sodium azide (50 mM) + light (660 nm 5 minutes 100 mW/cm^2)

- Ce6-MSN + light (660 nm 5 minutes 100 mW/cm^2)

The treatment groups were exposed to light after the two-hour incubation period. After the 24 hours, MTT was applied. Two independent repeats were performed.

3.12 Photodegradation Assessment under Light Irradiation

This experiment was carried out to compare the change in absorbance of free Ce6 and Ce6-MSN exposed the light irradiation. 10.8 μg/mL Ce6 and 50 μg/mL Ce6-MSN were used in this study. After each irradiation, absorbances at 660 nm were measured by UV-Vis spectrophotometer (ThermoScientific/Nanodrop 2000c). Absorbance values were evaluated at 0, 1.0, 2.5, 5.0, 10.0, 20.0 minutes.

3.13 Photodynamic Stability Experiment

The samples were prepared from previously determined concentrations in transparent falcon tubes and exposed to standard room light for the purpose of compare the photostability of Ce6 and Ce6-MSN. Four exposure times were used in the experiment: 0, 3, 7, and 14 days. The UV-Vis spectrophotometer was used to measure the sample's peak absorbance values to compare the values after each period. There were two distinct repetitions of the experiment.

3.14 Statistical Analysis

Statistical analysis was conducted utilizing a t-test for comparisons between two independent groups, and an Analysis of Variance (ANOVA) was employed for comparisons involving more than two groups, following the confirmation of Gaussian distribution. The program GraphPad Prism was used for all of the analyses.

4. RESULTS

4.1 Characterization of Nanoparticles

The distribution of the nanoparticle is shown in Figure 4.1. The average sizes were between 84 and 104 nm., in accordance with the DLS data displayed in this figure, which is in line with the MSN production methodology [38]. The synthesized MSNs appear as spherical in shape as in the image. The images and results show that MSNs are synthesized successfully in a homogeneous manner.

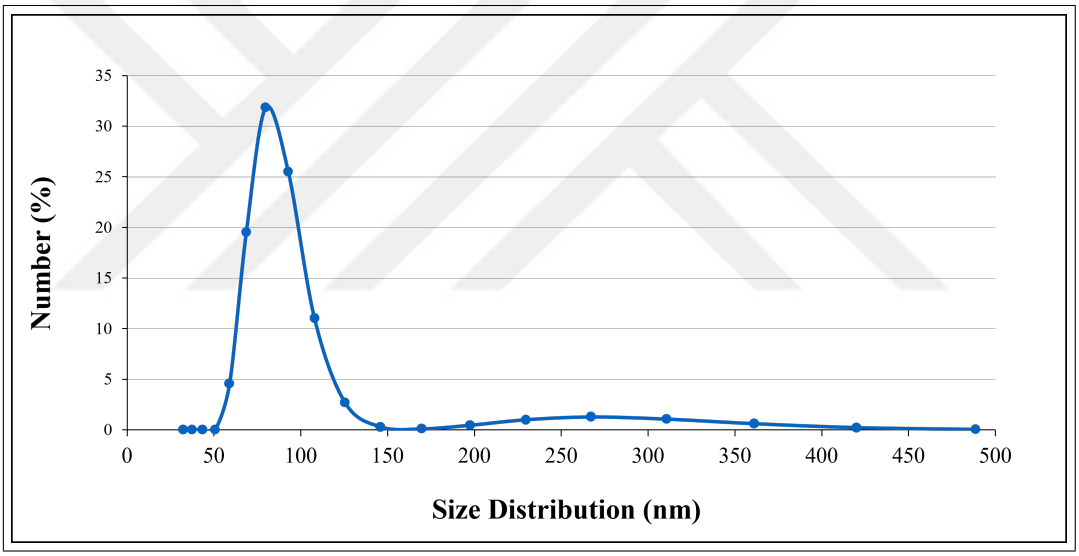

Figure 4.1 Size Distribution result of MSN.

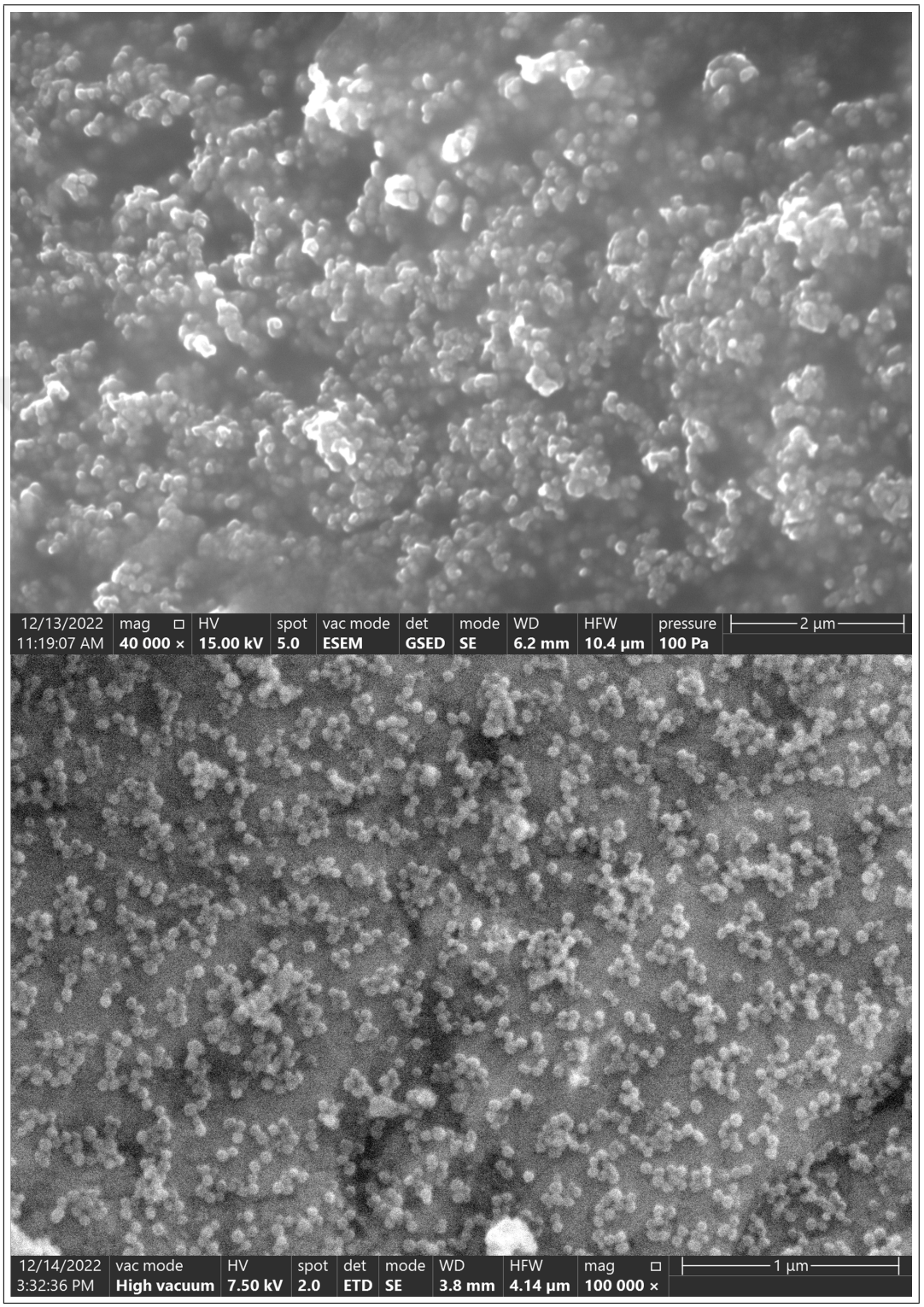

Figure 4.2 MSNs SEM images demonstrates the physical characterization.

4.2 Dark Toxicity Result

As seen in the Figure 4.3, Ce6-MSN starts to be toxic on A549 cells starting from 100 μg/mL. Therefore, 50 μg/mL, the highest non-toxic concentration was chosen for utilizing in this study's other experiments.

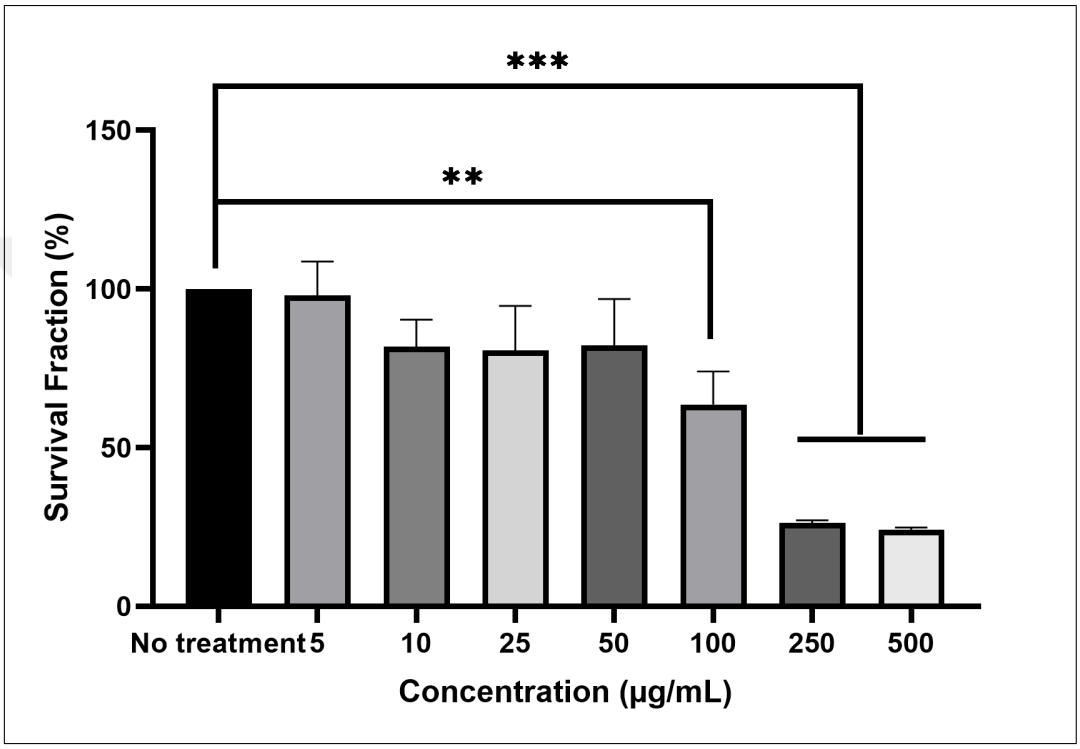

Figure 4.3 Results of MTT assay for A549 cells incubated with varying concentrations of Ce6-MSN. Every group's data was normalized with respect the corresponding no treatment value. Significant difference marked by (**) ($p < 0.01$). Significant difference marked by (***) ($p < 0.001$).

4.3 Determination of loaded amount of Ce6 into the Ce6-MSN

The amount of Ce6 in Ce6-MSN was calculated with the help of the standard curve generated using Ce6. Based on this curve, the amount of Ce6 in 50 μg/mL was found to be 10.8 μg/mL. The standard curve of Ce6 is shown in the Figure 4.4.

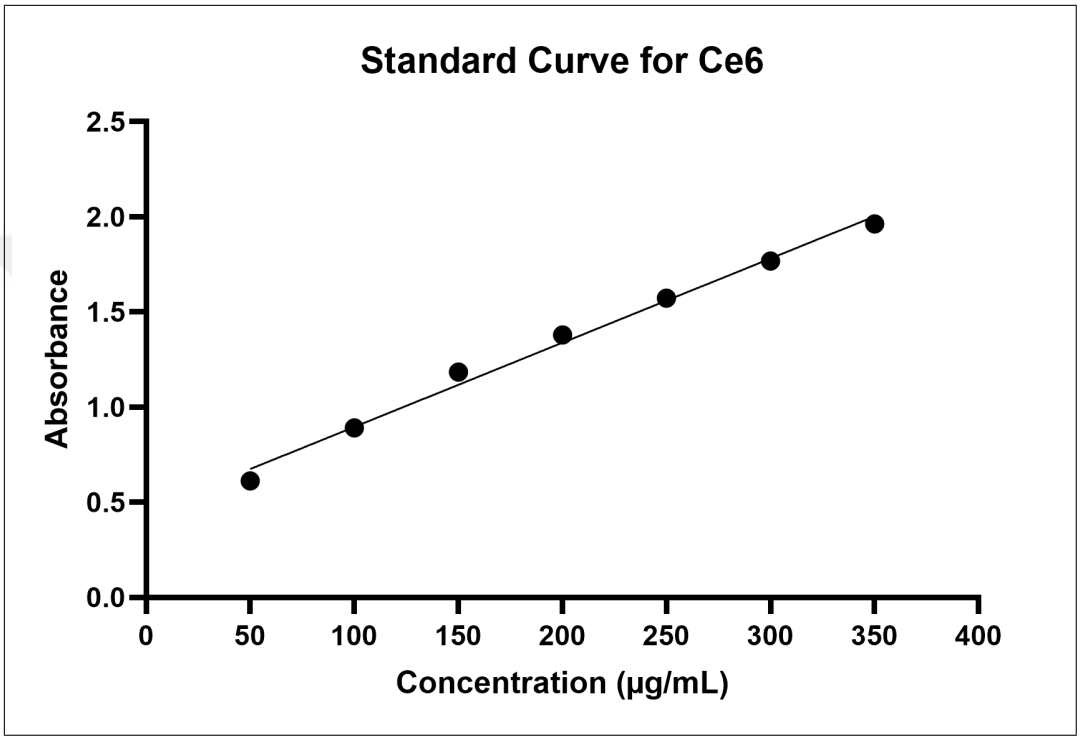

Figure 4.4 The standard curve of Ce6.

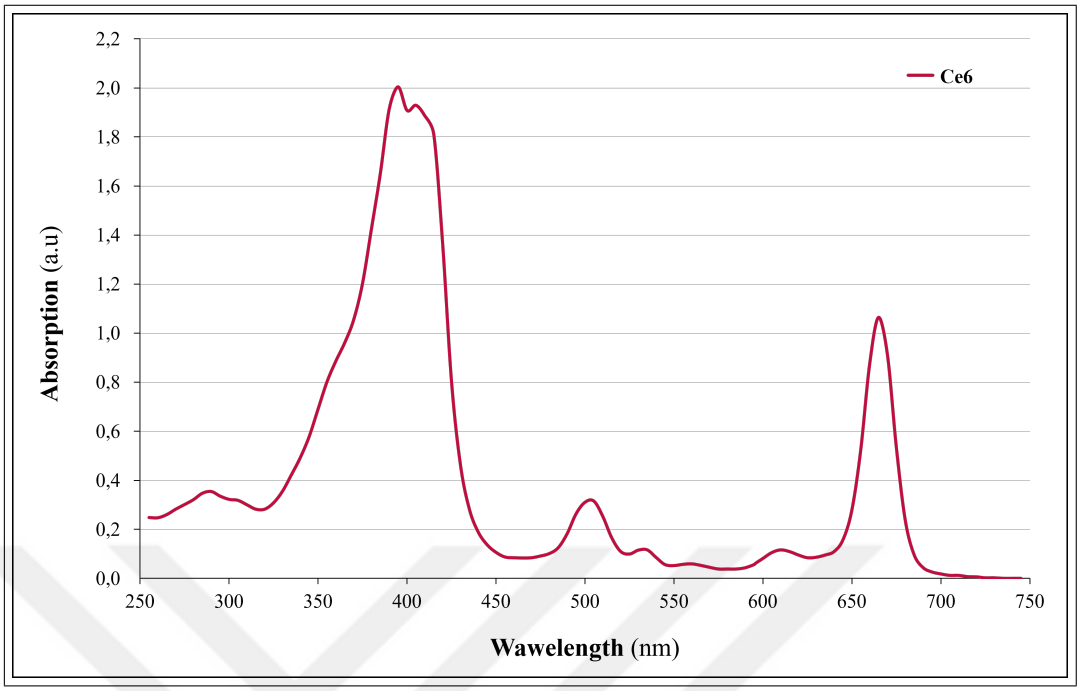

Figure 4.5 Absorbance spectrum of Ce6.

According to the absorption spectrum of Ce6 shown in Figure 4.5, a peak is seen at 660 nm. Apart from this, Ce6 and Ce6-MSN were loaded onto A549 and their dark toxicities were examined. When both groups were compared with no treatment group, no significant difference was found. This shows that the Ce6 concentration in MSNs that was calculated using the standard curve (10.8 μg/mL) was close to the actual concentration.

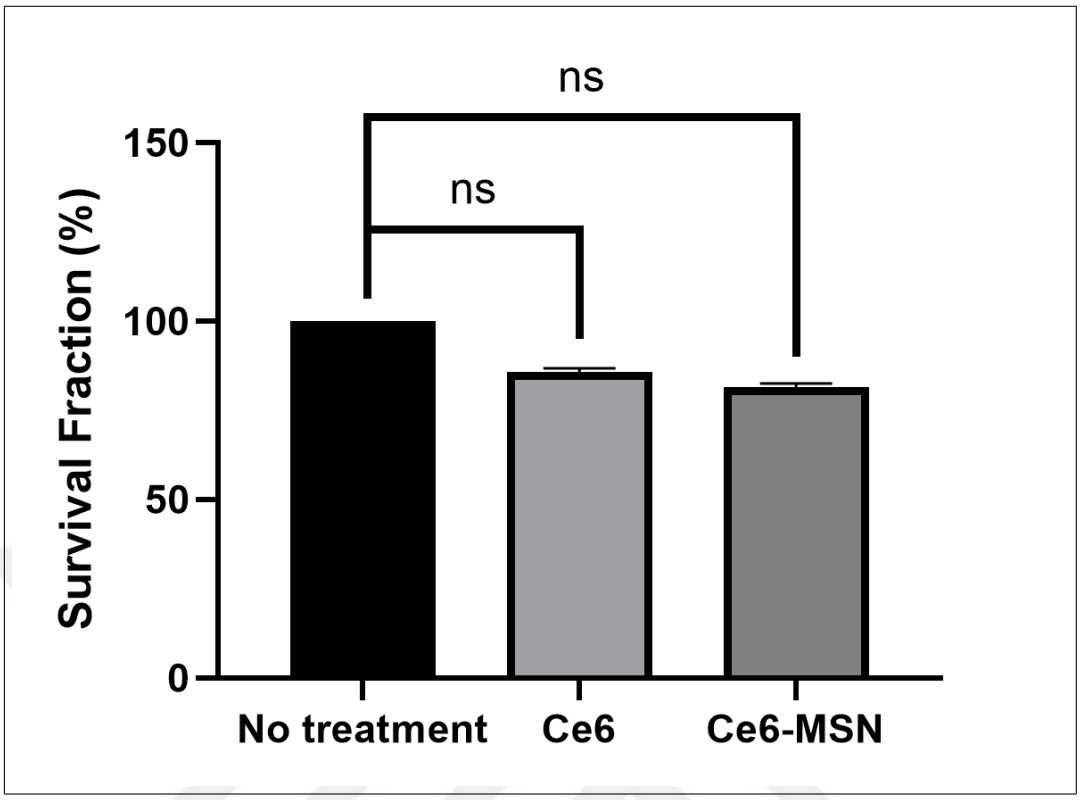

Figure 4.6 Dark toxicity results for A549 cells treated with Ce6 (10.8 μg/mL) and Ce6-MSN (50 μg/mL). Every group's data was normalized with respect to the corresponding no treatment value (ns:no significant difference).

4.4 PDT Experiment Result

Figure 4.7 demonstrates that, in comparison to no treatment and only light groups, cell irradiation with light at 660 nm wavelength and Ce6-MSN interaction causes significant cell death in A549 cells.

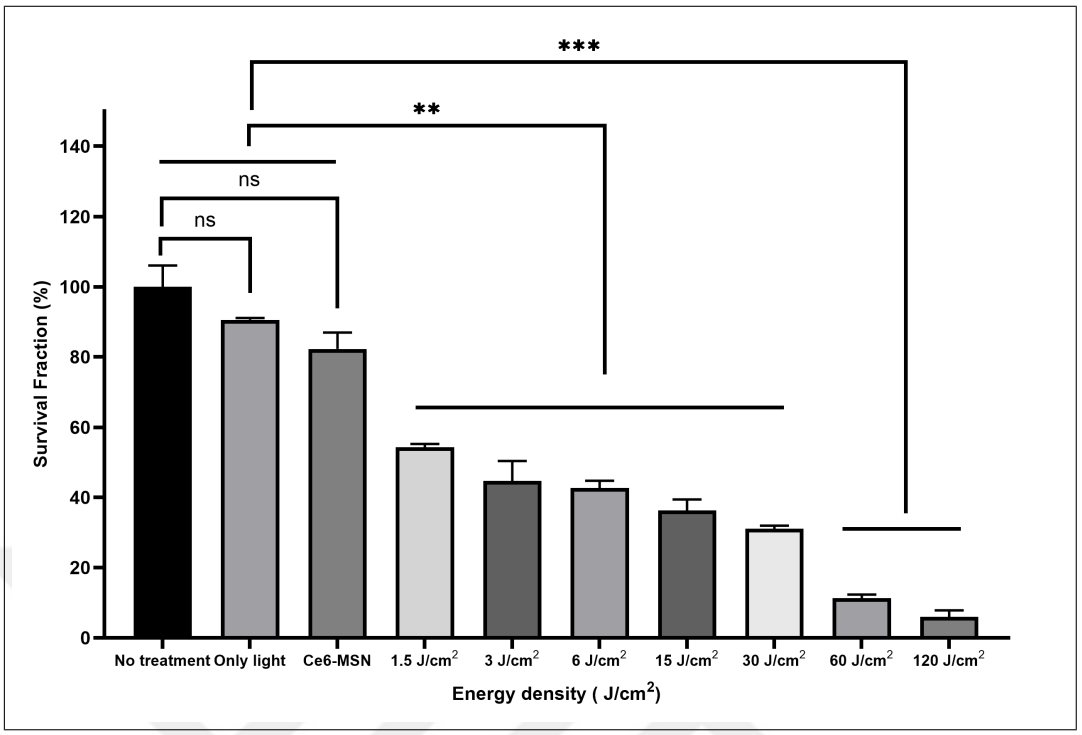

Figure 4.7 MTT assay results for A549 cells incubated with Ce6-MSN and light, only light and only Ce6-MSN. Light irradiation was performed with 100 mW/cm^2 and at 660 nm. Data for each group were normalized to the corresponding no treatment. Significant difference marked by (**) ($p < 0.01$). Significant difference marked by (***) ($p < 0.001$).

4.5 Comparison of PDT Efficacy of Free Ce6 and Ce6-MSN

Figure 4.8 illustrates that when free Ce6 and Ce6-MSN were loaded into A549 cells and 660 nm wavelength light was applied, a significant decrease in survival fraction was observed in both. Light exposure was applied for 1 minute for Ce6 and Ce6-MSN groups. Also, the two experimental groups did not show a statistical difference, which shows that Ce6-MSN is as effective as the free Ce6 in killing lung cancer cells.

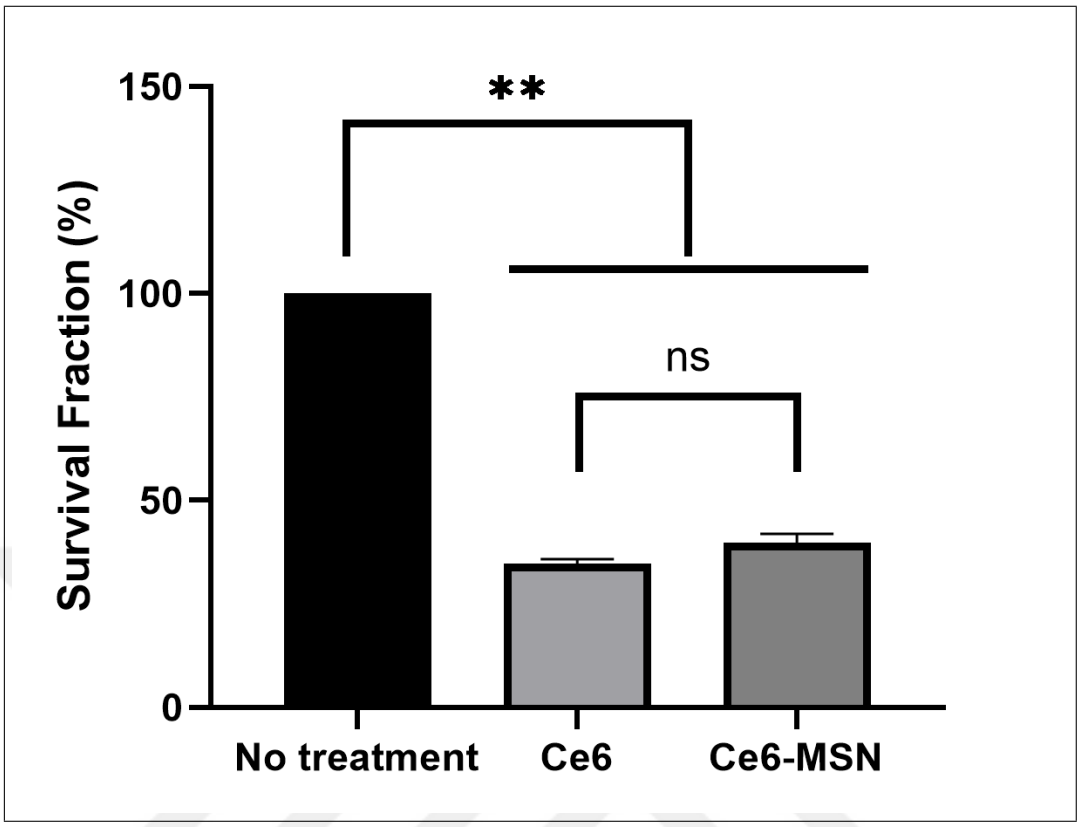

Figure 4.8 MTT assay results after the incubation of A549 cells with Ce6 and Ce6-MSN and light irradiation performed with 100 mW/cm^2 and at 660 nm. Each group was exposed to light for 1 minute. Significant difference marked by (**) ($p < 0.01$).

4.6 Cellular Uptake

Comparing Ce6-MSN nanoparticles to Ce6, Figure 4.9 demonstrates a considerable increase in the A549 cell's cellular uptake. According to the results, while free Ce6 is taken up into the cell by an average of 0.0000018 g/10^6, this number is an average of 0.0000075 g/10^6 for Ce6-MSN. Accordingly, we can say that when Ce6 is combined with MSN, cellular uptake is increased approximately 4-fold.

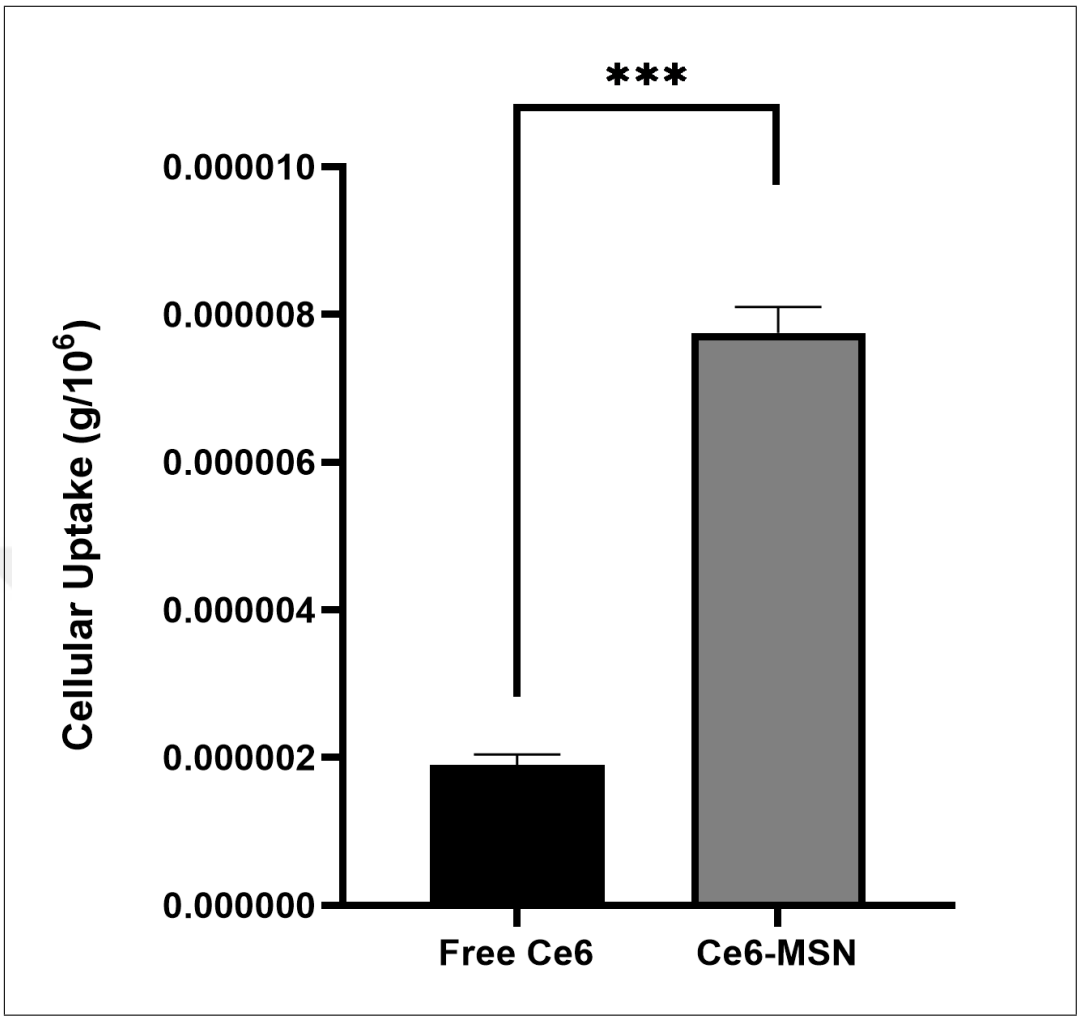

Figure 4.9 Cellular uptake results of Ce6 and Ce6-MSN.Significant difference marked by (***) (p =0.0007).

4.7 Primary Singlet Oxygen Mechanism

The experiment's findings demonstrate that 50 mM sodium azide has no cytotoxic effects on cells (Figure 4.10). The subsequent experiment, as shown in Figure 4.11, demonstrated that Ce6-MSN mediated PDT decreased the survival rate by approximately 63% when sodium azide was not in the cell. When sodium azide was present in the cell, the survival rate could decrease 25% with the same therapy. Results demonstrate that the effectiveness of Ce6-MSNs mediated PDT was dramatically reduced when $^1O_2$ was quenched with sodium azide.

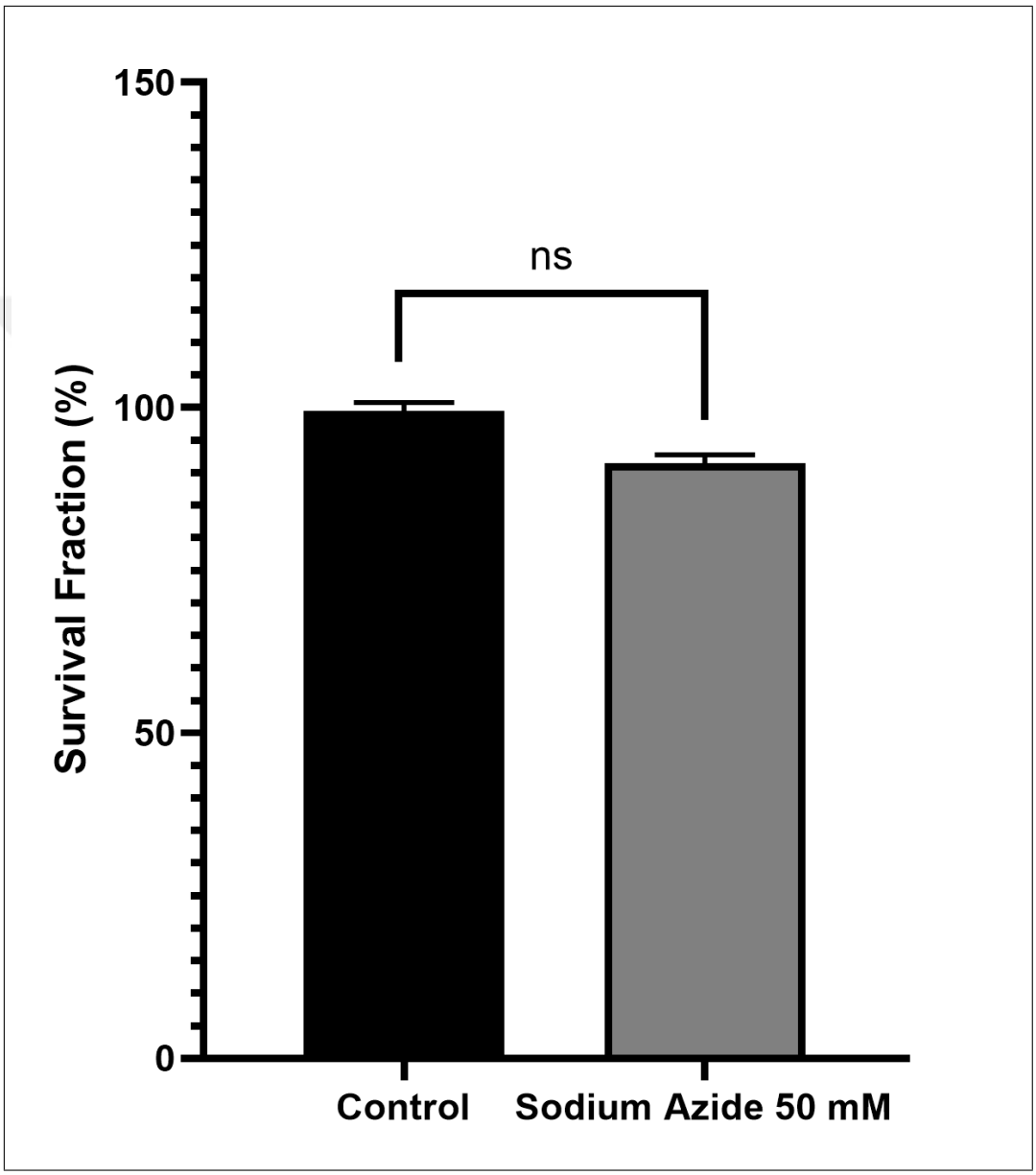

Figure 4.10 MTT assay results of 50 mM Sodium Azide in A-549 cells in dark condition. Data for the group were normalized to no treatment.

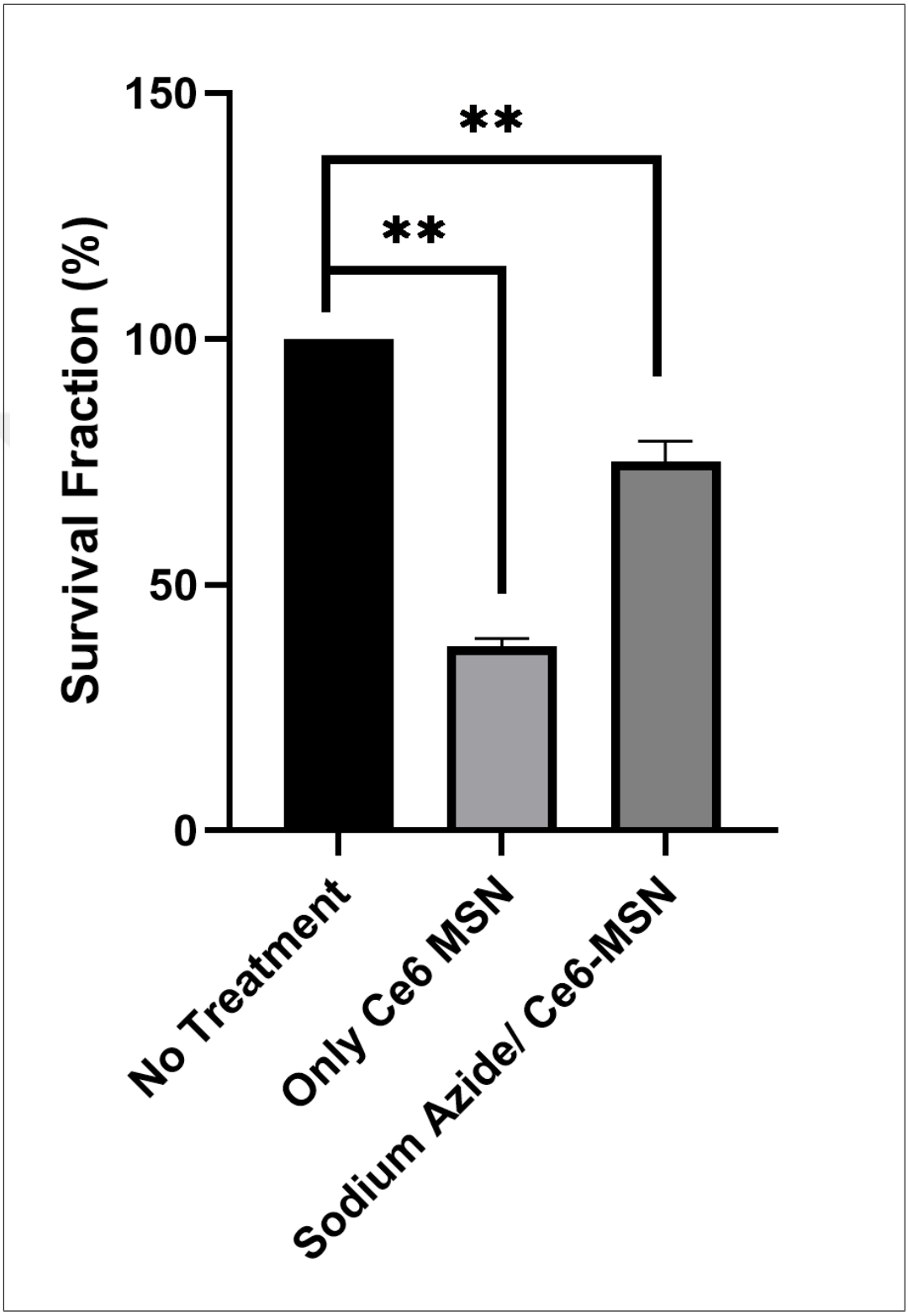

Figure 4.11 MTT assay results of A-549 cells after incubation with and without sodium azide, light irradiation performed with 100 mW/cm^2 and at 660 nm for 5 minutes. Data for each group were normalized to the corresponding untreated controls.Significant difference marked by (**) ($p < 0.01$).

4.8 Photodegradation Assessment Under Light Irradiation

The Figure 4.12 shows the absorbance change of Ce6 and Ce6-MSN at 660 nm with time. It was observed that the absorbance of free Ce6 changed from the first minute, but Ce6-MSN started to change from the 5th minute.

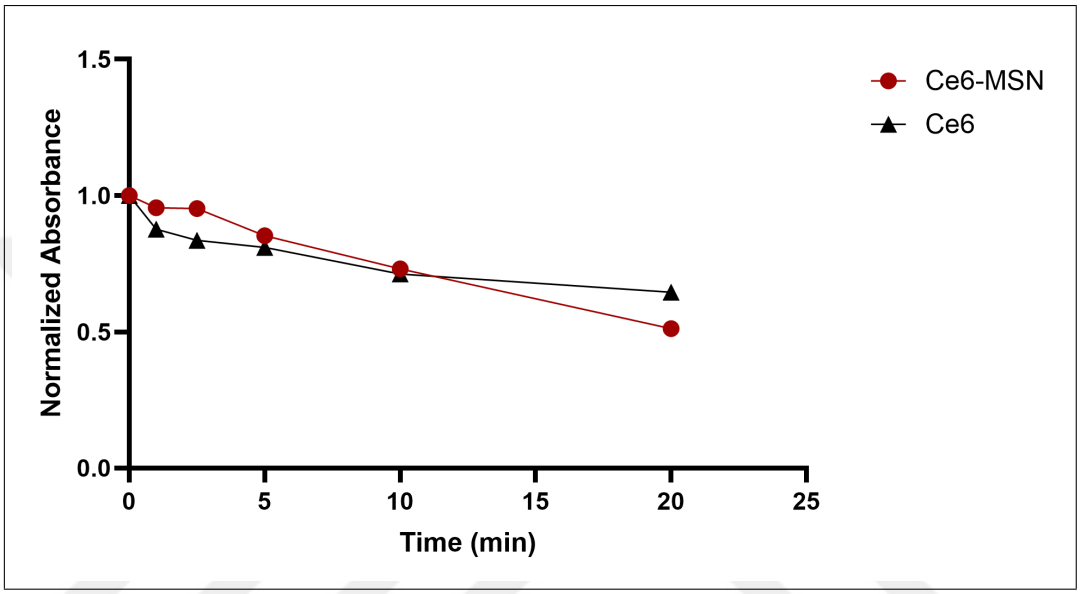

Figure 4.12 Absorbance change of Ce6 and Ce6-MSN under 660 nm with time.

4.9 Comparison of the photostability of free Ce6 and Ce6-MSN

Figures 4.13 show that the absorbance of both Ce6 and Ce6-MSN at 660 nm when exposed to room light for 14 days. It is seen that Ce6-MSN maintains its photostability until the 5th day and starts to decrease in the following days. Free Ce6, on the other hand, is seen to have a decreasing trend from the first day, although it experiences fluctuations.

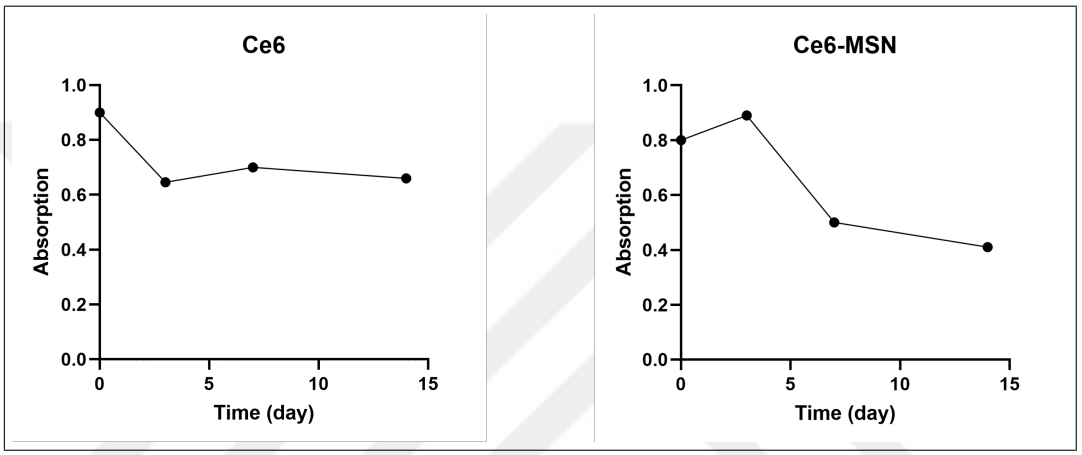

Figure 4.13 Photostability of Ce6 and Ce6-MSN during 14 days, absorbance at 660 nm.

5. DISCUSSION

Traditional cancer treatment approaches may fail or cause severe side effects. PDT, however, represents selective, minimally invasive method [43]. The therapeutic efficacy of PDT depends on the PS used, leading to extensive efforts to identify an optimal PS. Ce6, an FDA-approved second-generation PS, fulfills the essential clinical requirements for PDT. It has a high quantum yield (0.7), enhancing its effectiveness. Ce6 is renowned for its substantial ROS generation and its potent anticancer activity against various types of cancer [44].

Hydrophobicity is a significant limitation of Ce6, resulting in poor biodistribution and short circulation time. To address this issue, varies nanosystmes were developed to enhance the solubility of Ce6, thereby improving its bioavailability. Additionally, these nanosystems facilitate increased tumor accumulation through passive targeting [45].

This study evaluates the efficacy of Ce6-loaded MSNs for the treatment of A549 lung cancer cells. The investigation encompasses assessments of toxicity, stability, singlet oxygen generation, absorbance change under light and cellular uptake.

Up to 100 μg/mL, Ce6-MSN did not exhibit any cytotoxic effect on A-549 cells in dark toxicity experiments at different concentration. At this dose, the survival proportion decreased to 37%. Our dark toxicity experiments to demonstrate the compatibility of MSN-Ce6 in the absence of light are consistent with the literature [25]. The cells remained unaffected up to 100 μg/mL, as was evident. To avoid side effects, 50 μg/mL was chosen for PDT experiments. In PDT experiments using 660 nm LED light source at 100 mW/cm^2, a survival fraction of 31% was observed at 5 minutes. This is consistent with a similar study in the literature [28].

The main mechanism of PDT-mediated cell death can be identified using sodium

azide, a singlet oxygen quencher [46]. After being exposed to light, the Ce6-MSN and Sodium Azide/Ce6-MSN groups were compared in our study. The outcome demonstrated that, in comparison to cells treated with Sodium Azide/Ce6-MSNs, the survival fraction of cells treated with Ce6-MSNs was considerably lower. These findings demonstrated that the main cause of cell death was $^1O_2$, which is generated by Type II reactions. On the other hand, since sodium azide can not totally prevent cell death, it can be claimed that the Type I mechanism contributes to the formation of ROS.

Cellular uptake experiments showed that the cellular uptake of Ce6-MSN was significantly higher than free Ce6. In the study conducted by Gaber Abdel and colleagues, it is said that the difference in cellular uptake was clearly seen when Ce6 was conjugated to MSN. This shows that our study is in accordance with the literature [47].

Studies have been presented in the literature that demonstrate how using MSNs improves PS's photostability. It was attempted to prevent the aggregation of integrated molecules within MSN pores using APTES and create a homogeneous distribution. This surface modification provides a protective environment to Ce6, increases its photostability and thus increases the effectiveness of the treatment as a whole [48].

This study used Ce6-MSN as a PDT agent and focused on its efficacy in lung cancer cell lines. While the study's findings are in accordance with practice in literature, a more extensive investigation encompassing diverse cancer cell lines should be conducted to assess its application in PDT. Future studies will focus on other surface modifications of MSN for increasing cellular uptake and in vivo experiment endosomal escape efficiency.

6. CONCLUSION

Ce6 is an FDA-approved PS with promising features including high singlet oxygen quantum yield and biocompatibility. However, its low solubility in aqueous solutions and tumor selectivity limits Ce6's efficacy. Drug delivery systems, such as liposomes and MSNs are researched to increase the stability and circulation time of PSs. MSNs are additionally advantageous for light-based applications since they are optically transparent. This study aimed to evaluate MSN-incorporated Ce6 in terms of stability, cellular uptake, and PDT efficacy on an in vitro lung cancer model.

The results demonstrated that although the incorporation of Ce6 into MSN did not enhance stability, as indicated by similar decreases in the absorbance peak during irradiation or ambient conditions, this conjugation method increased the cellular uptake of Ce6. Singlet oxygen generation was also significantly higher in Ce6-MSN. However, the comparison of PDT efficacy between free Ce6 and Ce6-MSN did not show a significant difference. This may be because some of the ROS was generated within the pores of the MSNs and could not contribute to cytotoxicity. Our findings also indicated that the primary mechanism of PDT was singlet oxygen-mediated, with Type I reactions making only a minor contribution to the overall cytotoxicity.

In conclusion, this study has shown that MSN-based drug delivery systems can be used to increase the uptake and singlet oxygen generation efficacy of PSs in PDT applications. Future studies will focus on assessing other surface modification methods to increase stability and PS loading capacity, as well as testing the developed nanoconjugates in vivo.

REFERENCES

1. WHO, "World Health Organization available: www.who.int," 2023.
2. El-Hussein, Ahmed, et al. "A review of chemotherapy and photodynamic therapy for lung cancer treatment." *Anti-Cancer Agents in Medicinal Chemistry (Formerly Current Medicinal Chemistry-Anti-Cancer Agents)*, Vol. 21, no.2, pp. 149-161, 2021.
3. Sung, Hyuna, et al. "Global cancer statistics 2020: GLOBOCAN estimates of incidence and mortality worldwide for 36 cancers in 185 countries." CA: A Cancer Journal For Clinicians, Vol. 71, no.3, pp. 209-249, 2021.
4. Wang, J-J., K-F. Lei, and F. J. E. R. M. P. S. Han. "Tumor microenvironment: recent advances in various cancer treatments." *European Review for Medical & Pharmacological Sciences*, Vol.22, no.12, 2018.
5. Usuda, Jitsuo, et al. "Photodynamic therapy (PDT) for lung cancers." *Journal of Thoracic Oncology*, Vol.1, no.5, pp. 489-493, 2006.
6. Chilakamarthi, Ushasri, and Lingamallu Giribabu. "Photodynamic therapy: past, present and future." *The Chemical Record*, Vol.17, no.8, pp. 775-802, 2017.
7. Simone II, Charles B., and Keith A. Cengel. "Photodynamic therapy for lung cancer and malignant pleural mesothelioma." *Seminars In Oncology*, Vol.41, no.6, 2014.
8. Vrouenraets, M. B., Visser, G. W., Snow, G. B., and Van Dongen, G. A. "Basic principles, applications in oncology and improved selectivity of photodynamic therapy." *Anticancer Research*, Vol.23, no.1B, pp. 505-522, 2014.
9. Henderson, Barbara W."Photodynamic therapy: basic principles and clinical applications" *CRC Press*, 2020.
10. Agostinis, Patrizia, et al. "Photodynamic therapy of cancer: an update." *CA: A Cancer Journal For Clinicians*, Vol.61, no.4, pp.250-281, 2011.
11. Dougherty, Thomas J., et al. "Photodynamic therapy." *Journal of National Cancer Institute*, Vol.90, no.12, pp. 889-905, 1998.
12. Celli, Jonathan P., et al. "Imaging and photodynamic therapy: mechanisms, monitoring, and optimization." *Chemical Reviews*, Vol.110, no.5, pp. 2795-2838, 2010.
13. Lucena, Silvia Rocío, et al. "Combined treatments with photodynamic therapy for non-melanoma skin cancer." *International Journal of Molecular Sciences*, Vol.16, no.10, pp. 25912-25933, 2015.
14. Leiter, Amanda, Rajwanth R. Veluswamy, and Juan P. Wisnivesky. "The global burden of lung cancer: current status and future trends." *Nature Reviews Clinical Oncology*, Vol.20, no.9, pp. 624-639, 2023.
15. Leiter, Amanda, Rajwanth R. Veluswamy, and Juan P. Wisnivesky. "Pathology of Lung Cancer." *Clinics in Chest Medicine*, Vol.32, no.4, pp. 669-692, 2011.
16. Hammerschmidt, Stefan, and Hubert Wirtz. "Lung cancer: current diagnosis and treatment." *Deutsches Arzteblatt International*, Vol.106, no.49, pp. 809, 2009.
17. Lee, Junseok, et al. "Doxorubicin/Ce6-loaded nanoparticle coated with polymer via singlet oxygen-sensitive linker for photodynamically assisted chemotherapy." *Nanotheranostics*, Vol.1, no.2, pp. 196, 2017.

18. Agostinis, Patrizia, et al. "Photodynamic therapy of cancer: an update." *CA: A Cancer Journal for Clinicians*, Vol.61, no.4, pp. 250-281, 2011.

19. Dolmans, Dennis EJGJ, Dai Fukumura, and Rakesh K. Jain. "Photodynamic therapy for cancer." *Nature Reviews Cancer*, Vol.3, no.5, pp. 380-387, 2003.

20. Jiang, Wenqi, et al."The current status of photodynamic therapy in cancer treatment." *Cancers*, Vol.15, no.3, pp. 585, 2023.

21. Garcia-Diaz, Maria, Ying-Ying Huang, and Michael R. Hamblin. "Use of fluorescent probes for ROS to tease apart Type I and Type II photochemical pathways in photodynamic therapy." *Methods*, Vol.109, pp. 158-166, 2016.

22. Lan, Minhuan, et al. "Photosensitizers for photodynamic therapy." *Advanced Healthcare Materials*, Vol.8, no.13, pp. 1900132, 2019.

23. St Denis, T. G., and M. R. Hamblin. "Supramolecular drug delivery platforms in photodynamic therapy." *Applications of Nanoscience in Photomedicine*, pp. 465-485, 2015.

24. Hu, Jiahe, et al. "808 nm near-infrared light-excited UCNPs@ mSiO2-Ce6-GPC3 nanocomposites for photodynamic therapy in liver cancer." *International Journal of Nanomedicine*, pp. 10009-10021, 2019.

25. Bharathiraja, Subramaniyan, et al. "Chlorin e6 conjugated silica nanoparticles for targeted and effective photodynamic therapy." *Photodiagnosis and Photodynamic Therapy*, Vol.19, pp. 212-220, 2017.

26. Sheleg, S. V., Zhavrid, E. A., et al. "Photodynamic therapy with chlorin e6 for skin metastases of melanoma." *Photodermatology, Photoimmunology & Photomedicine*, Vol.20, no.1, pp. 21-26, 2004.

27. Li, Y., Yu, Y., Kang, L., and Lu, Y. "Effects of chlorin e6-mediated photodynamic therapy on human colon cancer SW480 cells." *International Journal of Clinical and Experimental Medicine*, Vol.7, no.12, pp. 4867, 2014.

28. Yang, J., Teng, Y., Fu, Y., and Zhang, C. "Chlorins e6 loaded silica nanoparticles coated with gastric cancer cell membrane for tumor specific photodynamic therapy of gastric cancer." *International Journal of Nanomedicine*, pp. 5061-5071, 2019.

29. Bharathiraja, S., Moorthy, M. S., et al. "Chlorin e6 conjugated silica nanoparticles for targeted and effective photodynamic therapy." *Photodiagnosis and Photodynamic Therapy*, pp. 212-220, 2017.

30. Zheng, Yilin, Li, Ziying, et al. "Nanoparticle-based drug delivery systems for controllable photodynamic cancer therapy." *European Journal of Pharmaceutical Sciences*, Vol.144, pp. 105213, 2020.

31. Lucky, Sasidharan Swarnalatha, Khee Chee Soo, and Yong Zhang. "Nanoparticles in photodynamic therapy." *Chemical Reviews*, Vol.115, no.4, pp. 1990-2042, 2015.

32. Youssef, Z., Jouan-Hureaux, V., Colombeau, et al. "Titania and silica nanoparticles coupled to Chlorin e6 for anti-cancer photodynamic therapy. " *Photodiagnosis and Photodynamic Therapy*, Vol.22, pp. 115-126, 2018.

33. Argyo, C., Weiss, V., Brauchle, C., and Bein, T. "Multifunctional mesoporous silica nanoparticles as a universal platform for drug delivery." *Chemistry of Materials*, Vol.26, no.1, pp. 435-451, 2014.

34. Bayir, S., Barras, A., Boukherroub, et al. "Mesoporous silica nanoparticles in recent photodynamic therapy applications." *Photochemical & Photobiological Sciences*, Vol.17, pp. 1651-1674, 2018.

35. Prieto-Montero, R., Arbeloa, T., and Martinez-Martinez, V. "Photosensitizer-Mesoporous Silica Nanoparticles Combination for Enhanced Photodynamic Therapy. " *Photochemistry and Photobiology*, Vol.99, no.3, pp. 882-900, 2023.

36. Park, S., Park, H., Jeong, et al. "Hyaluronic Acid-Conjugated Mesoporous Silica Nanoparticles Loaded with Dual Anticancer Agents for Chemophotodynamic Cancer Therapy." *Journal of Nanomaterials*, Vol.2019, no.1, pp. 3481397, 2019.

37. Sun, J. H., Zhang, W., Zhang, D. Y., Shen, et al."Multifunctional mesoporous silica nanoparticles as efficient transporters of doxorubicin and chlorin e6 for chemophotodynamic combinatorial cancer therapy." *Journal of Biomaterials Applications*, Vol.32, no.9, pp. 1253-1264, 2018.

38. Lin, Y.-S., and C. L. Haynes "Impacts of mesoporous silica nanoparticle size, pore ordering, and pore integrity on hemolytic activity," *Journal of the American Chemical Society*, Vol.132, no.13, pp. 4834-4842, 2010.

39. Couleaud, P., Bechet, D., Vanderesse, et al. "Functionalized silica-based nanoparticles for photodynamic therapy." *Nanomedicine*, Vol.6, no.6, pp. 995-1009, 2011.

40. Stetefeld, J., McKenna, S. A., and Patel, T. R. "Dynamic light scattering: a practical guide and applications in biomedical sciences." *Biophysical Reviews*, Vol.8, pp. 409-427, 2016.

41. Liu, W., Tian, Y., Zhang, et al. "Timely coordinated phototherapy mediated by mesoporous organosilica coated triangular gold nanoprisms." *Journal of Materials Chemistry B*, Vol.6, no.23, pp. 3865-3875, 2018.

42. Sakuma, S., Otake, E., Torii, et al."Photodynamic therapy with glycoconjugated chlorin photosensitizer." *Journal of Porphyrins and Phthalocyanines*, Vol.17, no.05, pp. 331-342, 2013.

43. Wang, K., Zhang, Y., Wang, et al. "Self-assembled IR780-loaded transferrin nanoparticles as an imaging, targeting and PDT/PTT agent for cancer therapy." *Scientific Reports*, Vol.6, no.1, pp. 27421, 2016.

44. Liao, S., Cai, M., Zhu, et al. "Antitumor effect of photodynamic therapy/sonodynamic therapy/sono-photodynamic therapy of chlorin e6 and other applications." *Molecular Pharmaceutics*, Vol.20, no.2, pp. 875-885, 2023.

45. Hak, A., Ali, M. S., Sankaranarayanan, et al. "Chlorin e6: a promising photosensitizer in photo-based cancer nanomedicine." *ACS Applied Bio Materials*, Vol.6, no.2, pp. 349-364, 2023.

46. Huang, L., Xuan, Y., Koide, Y., Zhiyentayev, Tanaka, et al. "Type I and Type II mechanisms of antimicrobial photodynamic therapy: an in vitro study on gram-negative and gram-positive bacteria." *Lasers in Surgery and Medicine*, Vol.44, no.6, pp. 490-499, 2012.

47. Abdel Gaber, S. A., Stepp, H., et al. "Mesoporous silica nanoparticles boost aggressive cancer response to hydrophilic chlorin e6-mediated photodynamic therapy." *Cancer Nanotechnology*, Vol.14, no.1, pp. 67, 2023.

48. Wang, Y., Sun, Y., et al. "Charge-reversal APTES-modified mesoporous silica nanoparticles with high drug loading and release controllability." *ACS Applied Materials & Interfaces*, Vol.8, no.27, pp. 17166-17175, 2016.